US Army Corps
of Engineers
Construction Engineering
Research Laboratory

TECHNICAL REPORT M-354
July 1984

THE EFFECT OF FLUIDS ON WAVEGUIDES BELOW CUTOFF PENETRATIONS AS RELATED TO ELECTROMAGNETIC SHIELDING EFFECTIVENESS

by
Michael K. McInerney
Scott Ray
Ray McCormack
Steve Castillo
Raj Mittra

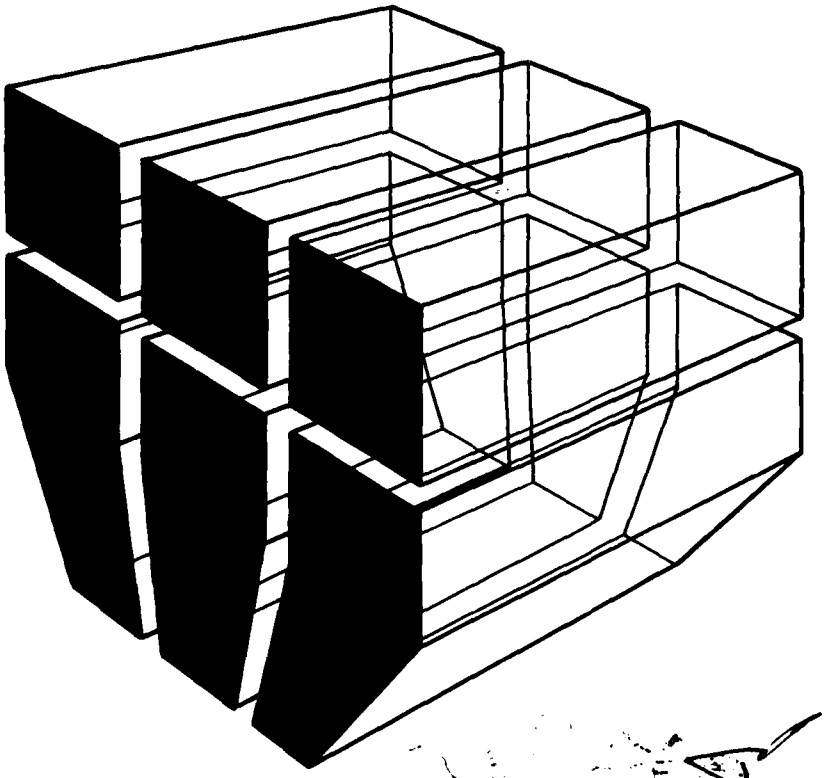

Approved for public release; distribution unlimited.

UNCLASSIFIED

SECURITY CLASSIFICATION OF THIS PAGE *(When Data Entered)*

REPORT DOCUMENTATION PAGE	READ INSTRUCTIONS BEFORE COMPLETING FORM
1. REPORT NUMBER: ~~USA~~-CERL TR M-354	2. GOVT ACCESSION NO.: AD-A144 685 / 3. RECIPIENT'S CATALOG NUMBER:
4. TITLE *(and Subtitle)*: THE EFFECT OF FLUIDS ON WAVEGUIDES BELOW CUTOFF PENETRATIONS AS RELATED TO ELECTROMAGNETIC SHIELDING EFFECTIVENESS	5. TYPE OF REPORT & PERIOD COVERED: FINAL 6. PERFORMING ORG. REPORT NUMBER:
7. AUTHOR(s): Michael K. McInerney, Steve Castillo, Scott Ray, Raj Mittra, Ray McCormack	8. CONTRACT OR GRANT NUMBER(s): MIPR-82-577
9. PERFORMING ORGANIZATION NAME AND ADDRESS: U.S. Army Construction Engr Research Laboratory, P.O. Box 4005, Champaign, Il 61820-1305	10. PROGRAM ELEMENT, PROJECT, TASK AREA & WORK UNIT NUMBERS:
11. CONTROLLING OFFICE NAME AND ADDRESS	12. REPORT DATE: July 1984 13. NUMBER OF PAGES: 62
14. MONITORING AGENCY NAME & ADDRESS *(if different from Controlling Office)*	15. SECURITY CLASS. *(of this report)*: UNCLASSIFIED 15a. DECLASSIFICATION/DOWNGRADING SCHEDULE

16. DISTRIBUTION STATEMENT *(of this Report)*
Approved for public release; distribution unlimited

17. DISTRIBUTION STATEMENT *(of the abstract entered in Block 20, if different from Report)*

18. SUPPLEMENTARY NOTES
Copies are available from the National Technical Information Service
Springfield, VA 22161

19. KEY WORDS *(Continue on reverse side if necessary and identify by block number)*
electromagnetic shielding
waveguides
fluids
pipes

20. ABSTRACT *(Continue on reverse side if necessary and identify by block number)*

This study investigates the effect of fluid/loading on a waveguide below cutoff penetration through electromagnetic shields. The study addresses waveguide mode excitations, electromagnetic wave attenuation within the fluid-filled waveguide, and the effect of the waveguide on electromagnetic shielding effectiveness as measured by test procedures like those outlined in MIL-STD-285. Design curves are presented for commonly used pipe sizes and for some fluids that may be required to pass through electromagnetic shields. Results →

DD FORM 1 JAN 73 1473 EDITION OF 1 NOV 65 IS OBSOLETE

UNCLASSIFIED

SECURITY CLASSIFICATION OF THIS PAGE *(When Data Entered)*

BLOCK 20. (Cont'd)

show expected changes in cutoff frequency due to variation in dielectric constant and response variations due to changes in loss tangent with frequency.

FOREWORD

This investigation was performed for the Defense Nuclear Agency, EMP Effects Division, Washington, DC, under contract no. MIPR 82-577. The DNA project officer was LTC R. Blair Williams.

The study was done by the Engineering and Materials (EM) Division, U.S. Army Construction Engineering Research Laboratory (CERL). Other CERL personnel directly involved in the study were Roy Axford and John Clements.

Dr. Robert Quattrone is Chief of EM. COL Paul J. Theuer is Commander and Director of CERL, and Dr. L. R. Shaffer is Technical Director.

CONTENTS

TABLES

FIGURES

FIGURES (Cont'd)

THE EFFECT OF FLUIDS ON WAVEGUIDES BELOW CUTOFF PENETRATIONS AS RELATED TO ELECTROMAGNETIC SHIELDING EFFECTIVENESS

1 INTRODUCTION

Background

It is common practice in electromagnetic pulse (EMP) and electromagnetic interference (EMI) hardened facilities that house sensitive electronic equipment to enclose part or all of the facility in a metallic electromagnetic shield. This shield must have openings for personnel and equipment access, electric power entry, communications and control cooling, heating, ventilating, air-conditioning (HVAC), and entry of various fluids such as water and refrigerants. Technology for the design of these penetrations is, in general, highly advanced and is discussed in numerous technical manuals and design handbooks.[1]

When it is required to bring fluids through a shield, it must be done in a manner which does not compromise the shield. One approach is to use a completely closed metallic piping or conduit system into which compromising electromagnetic energy cannot enter. The metallic pipe or conduit typically is welded or otherwise electrically connected around its periphery to the shield at the point of entry.

Another approach is to use a short length of metallic pipe to penetrate the shield. This length of pipe acts as a waveguide below cutoff, blocking unwanted electromagnetic energy. (A waveguide passes only those frequencies above a particular "cutoff" frequency.) This technique is used to isolate the pipe ground from the shield ground without compromising the shield. It also permits the connection of nonmetallic pipes to the shield without a loss in shielding.

A honeycomb grating is an extension of the waveguide below cutoff concept. A honeycomb grating is made of many tubular cells with hexagonal cross sections. Each cell acts as a waveguide below cutoff.

Typically, when designing shield penetrations, the pipes are assumed to be air-filled. In practice, however, it is often necessary to bring fluids other than air through the pipes. Examples are tapwater, distilled water, fuel, refrigerants, fire extinguishing fluids, and freeze prevention fluids. These fluids may have relative dielectric constants and dissipation factors

[1] DASA EMP Handbook, DASA 2114-1 (Defense Atomic Support Agency [DASA] Information and Analysis Center, September 1968); DNA EMP Awareness Course Notes, Third Ed, DNA 2772T (Defense Nuclear Agency, October 1977); EMP Engineering Practices Handbook, NATO file No. 1460-2 (October 1977); Nuclear Electromagnetic Pulse (NEMP) Protection, TM 5-855-5 (Headquarters, Department of the Army, February 1974).

much different from air. The attenuation of the electromagnetic energy propagating within the fluid-filled pipe will be different from that of the air-filled pipe.

In acceptance testing of EMI and EMP hardened facilities, the pipe penetrations usually are checked using the techniques defined in MIL-STD 285 or IEEE 299.[2] These methods use horn antennas or open waveguide antennas to measure the shielding effectiveness. Measurement is relatively straightforward for a simple shield but becomes more complicated when the shield has penetrations. Some antenna positions required by IEEE 299 cannot be achieved because the external piping connected to the shield prevents positioning of the test antennas on the pipe axis. The same is true for some honeycomb gratings.

Clearly, fluid-filled pipes penetrating a shielded enclosure have special design requirements. Designers of EMI or EMP shields therefore need specific data to assist in designing fluid penetrations.

Objective

The objectives of this study were to:

1. Perform a mathematical analysis of waveguides and honeycomb filters to determine attenuation versus frequency.

2. Provide design curves showing cutoff frequency and attenuation versus frequency for commonly used pipe sizes and fluids.

3. Verify the above solutions empirically.

Approach

A literature search was performed to obtain information on related work covering energy capture ratios for open waveguides, measurement of electromagentic parameters of fluids, and performance of honeycomb filters. Computer programs were developed to calculate the waveguide's performance when fluid-filled. Laboratory testing was performed on representative waveguides to verify analytical methods. Analysis was performed to calculate the shielding effectiveness of honeycomb filters.

Mode of Technology Transfer

It recommended that the results of this study be incorporated in the Defense Nuclear Agency's EMP Engineering Practices Handbook for Facilities

[2] Method of Attenuation Measurements for Enclosures, Electro-Magnetic Shielding, for Electronic Test Purposes, MIL-STD 285 (Department of Defense, July 1956); Measurement of Shielding Effectiveness of High-Performance Shielding Enclosures, Institute of Electrical and Electronic Engineers (IEEE) Method 299, (1975).

which is in preparation. It is also recommended that these results be included in Army Technical Manual (TM) 5-855-5, Nuclear Electromagnetic Pulse (NEMP) Protection.

2 THEORY AND PROCEDURE

Introduction

This chapter describes the analysis of a dielectric loaded waveguide. Specifically, the modes excited in a waveguide by an incident plane wave and the accuracy of shielding tests such as IEEE 299 and MIL-STD-285 are addressed. An experimental verification for the theoretical analysis of the loaded waveguide is included.

A waveguide is a hollow metallic pipe (usually circular or rectangular) through which electromagnetic energy propagates. The most important waveguide parameter is its cutoff frequency, that is, the frequency at which the waveguide starts dissipating the electromagnetic energy instead of propagating it. Frequencies above cutoff are passed through the waveguide with no attenuation. Frequencies below cutoff are heavily attenuated within the waveguide.

The waveguide cutoff frequency is a function of the waveguide cross sectional area and the contents of the waveguide. The larger the cross sectional area, the lower the cutoff frequency. Generally, any fluid in the waveguide besides air will have a lower cutoff frequency than the air-filled waveguide.

A waveguide below cutoff penetration of a shield consists of a length of metal pipe passing through the shield. Where the pipe penetrates the shield, the pipe periphery is electrically connected to the shield.

Waveguide below cutoff penetrations are used in plastic pipe systems to block unwanted electromagnetic energy. They are also used to eliminate ground loops.

In most shielded facilities, numerous piping and conduit penetrations will be required, possibly at widely spaced points. The piping and conduit outside the shield act as electromagnetic energy collectors. Many of these pipes and conduits pass underground and thus are earth-grounded. The use of many earth-grounded piping systems with shield penetrations creates electromagnetic energy collecting ground loops. These ground loops are not consistent with optimized grounding system philosophy, so it may be necessary to electrically disconnect the piping system from the shield. This is commonly done by inserting nonmetallic pipe sections near the shield, then penetrating the shield with a waveguide below cutoff piping section.

Circular Waveguide Theory

Figure 1 shows the basic geometry of a pipe penetrating a shielded enclosure. The pipe has inside diameter d and length L. It contains a fluid with relative dielectric constant ε_r and loss tangent tan δ. A plane wave is incident from the left, propagating along the z-axis.

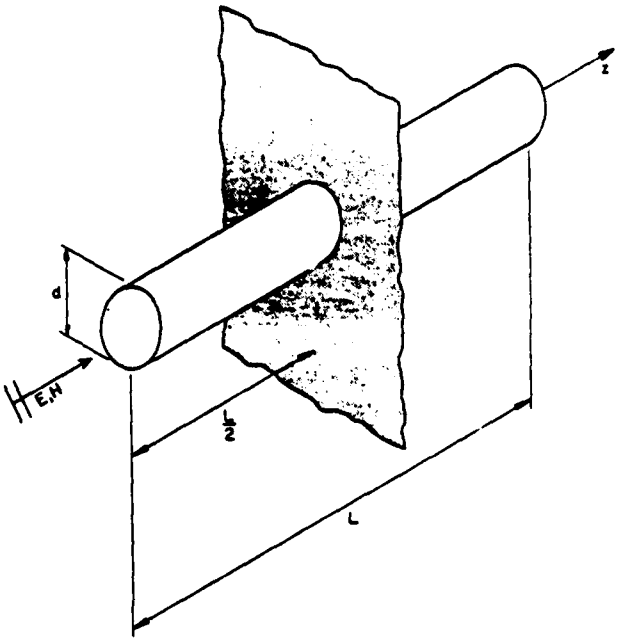

Figure 1. Geometry of pipe penetrating a shield.

A rigorous analysis of the electromagnetic energy coupled into the pipe and then into the enclosure is difficult. Because the relative dielectric constants, loss tangents, frequencies, and pipe dimensions vary widely, several types of analysis are required. Most importantly, a rigorous multimodal examination of the problem would require precise knowledge of the excitation mechanism.

The forms of excitation found in practice are likely to vary widely and would most certainly differ from the basic geometry just described. Because of this difference, an approximate transverse electric and magnetic fields (TEM)-waveguide analysis is used to obtain the shielding effectiveness of the pipe alone. Inclusion of a particular excitation mechanism would increase shielding effectiveness because the coupling of the incident wave to the pipe is imperfect.

Appendix A presents the basic equations for the analysis of electromagnetic wave propagation through a circular waveguide (pipe).

Modes Excited in a Circular Waveguide

Typically, most of the energy in a waveguide is carried in the first few propagating modes. This was observed during the tests conducted for this report.

Figure 2 is a plot of energy propagation through a 1.5-in. (3.81-cm) inside diameter (i.d.) pipe as a function of frequency. The pipe was excited by a plane wave as shown in Figure 1. The vertical scale represents the attenuation resulting from the pipe relative to free space.

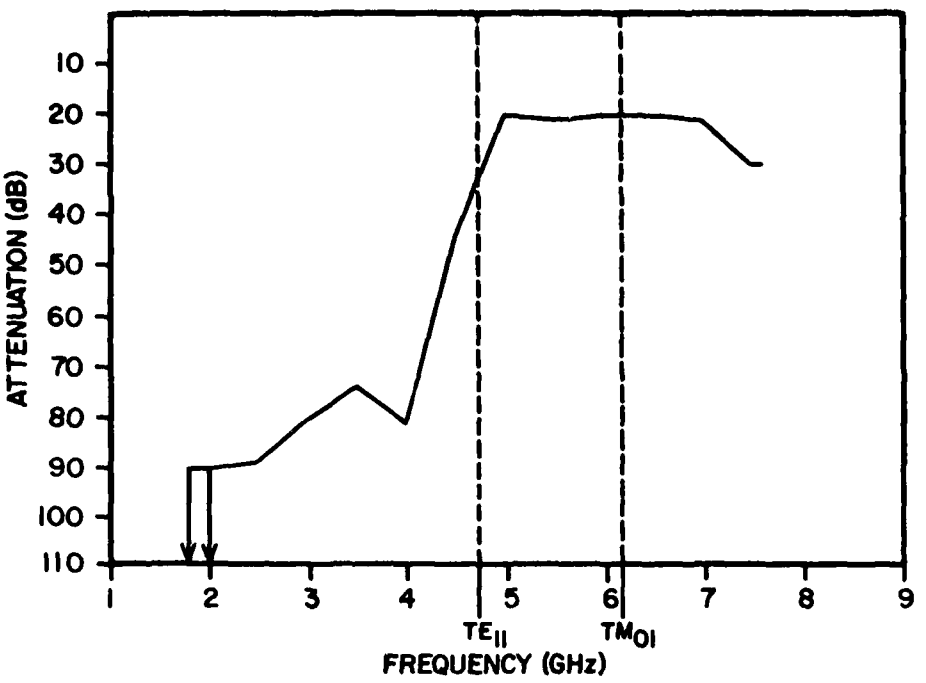

Figure 2. Transmission through an air-filled 1.5-in. (3.8-cm) i.d. pipe.

For an air-filled pipe, the two lowest modes are the TE_{11} and TM_{01} modes with cutoff frequencies of 4.7 and 6.14 GHz, respectively. Figure 2 clearly shows that the TE_{11} must be present. Also, there is no significant increase in the power transferred above the TM_{01} cutoff frequency, indicating that most of the energy is coupled into the TE_{11} mode.

Computer Model of a Circular Waveguide

Appendix C contains listings and descriptions of two FORTRAN V programs, Pipe 1A and Pipe 1B (Figures C1 and C2), that compute the theoretical attenuation resulting from a length of pipe. Both programs are designed for use on an interactive computer system. The frequency and corresponding attenuation are written into a named file for storage. The user is questioned for the problem parameters.

Program Pipe 1A computes the attenuation over a band of frequencies. The relative dielectric constant and loss tangent are assumed to be constant over this band. The variables to be entered are: pipe inside radius, pipe length, relative dielectric constant, loss tangent, minimum frequency in band, maximum frequency in band, the frequency increment to be used within the band, and the name of the output file in which the results are to be stored.

Program Pipe 1B computes the attenuation for a particular frequency. The program is cyclical so the attenuation at any number of frequencies may be computed. However, the pipe inside radius and pipe length are entered only once. The parameters to be entered are: pipe inside radius, pipe length, the name of the output file in which the results are to be stored, frequency 1,

relative dielectric constant 1, loss tangent 1, frequency 2, relative dielectric constant 2, loss tangent 2, frequency 3, ...

Experimental Verification

A crude verification of the theoretical waveguide attenuation was performed. The experimental set-up is shown in Figure 3. The system consists of a 6-in. (15.25-cm) pipe penetrating a shielded enclosure. The pipe inside diameter is 1.48 in. (3.76 cm). The ends of the pipe were covered with plastic wrap so the pipe could be filled with fluid. The receiver and its horn antenna were placed inside the shielded enclosure. The signal generator and transmitting horn (identical to the receiving horn) were placed outside the enclosure. The distance between each horn and the nearest end of the pipe was 12 in. (30.48 cm), resulting in an overall horn separation of 30 in. (76.20 cm) (12 + 6 + 12). Free-space reference measurements were taken with both horns outside the enclosure spaced 30 in. (76.20 cm) apart.

Measurements were taken between 2.5 and 7.5 GHz with a 0.5-GHz spacing. An additional measurement was made at 7.6 GHz. This narrow test band was a result of equipment limitations. (The horns could not be used below 2.5 GHz and the transmitter could not be used above 7.6 GHz.)

Incident wave power is lost not only in the waveguide but also at the free space-pipe interfaces. The power is lost at these interfaces because of coupling. Therefore, to verify the waveguide attenuation, the coupling loss must also be determined.

It is best to measure the coupling loss as it represents the loss due to a particular waveguide excitation mechanism. Also, since excitation mechanisms vary widely depending on geometry, nearby metallic objects, and wave type, it is more practical to measure coupling loss.

The measurement of coupling loss is simple for frequencies above cutoff. The wave will not be attenuated within an air-filled pipe. Therefore, the difference between the free space reference measurement and the measurement for the air-filled pipe will be the coupling loss.

For frequencies below cutoff, the measurement of coupling loss is dependent on the wave attenuation within the pipe. For this reason, a theoretical method was used to determine the coupling loss. Appendix B describes the calculation of coupling loss using antenna directivities. Table 1 lists the computed and measured coupling losses for the experimental set-up of Figure 3.

Four fluids covering a wide range of relative dielectric constants were used in the test: air ($\varepsilon_r = 1$), carbon tetrachloride ($\varepsilon_r \approx 2$), methanol ($\varepsilon_r \approx 24$), and distilled water ($\varepsilon_r \approx 63$). Tables 2 through 4 list results of the test. For methanol and distilled water, the frequency band was limited because of high waveguide attenuation (-90 dBm was the minimum receiver sensitivity).

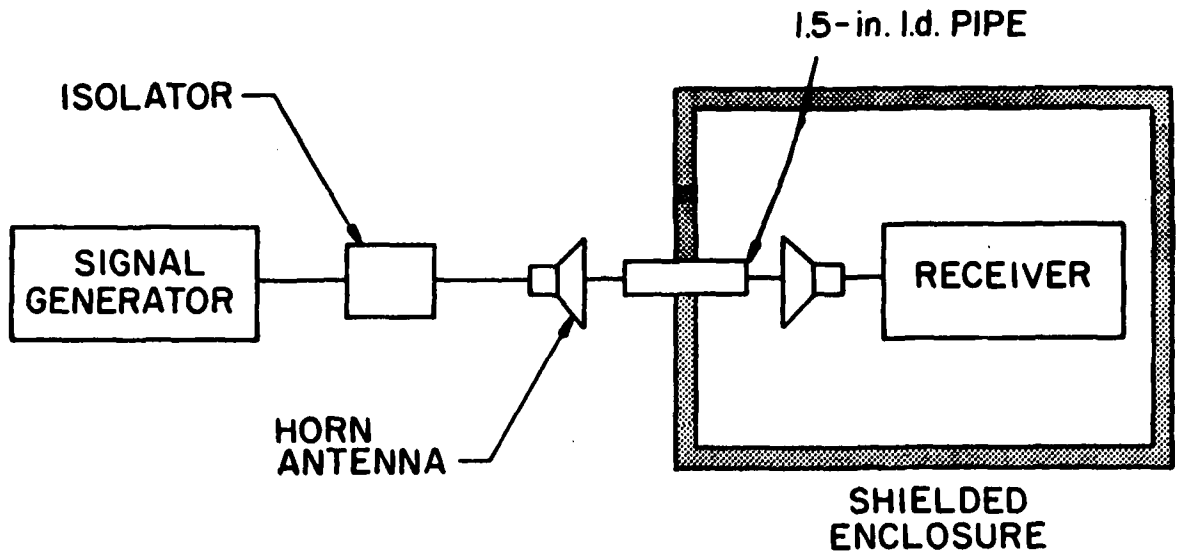

Figure 3. Measurement setup for waveguide below cutoff verification.

Table 1

Coupling Loss Versus Frequency for a 1.5-In. i.d. Pipe

Frequency (GHz)	Coupling Loss (dB)
2.5	24
3.0	22
3.5	21
4.0	20
4.5	19
5.0	18*
5.5	14*
6.0	24*
6.5	11*
7.0	13*
7.5	24*
7.6	32*

*Determined experimentally.

Table 2

Transmission Loss Through 1.5-In. i.d. Pipe Filled With Carbon Tetrachloride

Frequency (GHz)	Free-space reference (dB)	Theoretical attenuation in pipe (dB)	Coupling loss (dB)	Computed measurement	Actual measurement
2.5	-5	81	24	-110	-79
3.0	13	44	22	-53	-37
3.5	11	0	21	-10	- 8
4.0	7	0	20	-13	- 8
4.5	7	0	19	-12	- 8
5.0	7	0	18	-11	-11
5.5	2	0	14	-12	-12
6.0	12	0	24	-12	-13
6.5	-7	0	11	-18	-19
7.0	-19	0	13	-32	-33
7.5	-15	0	24	-39	-38
7.6	-11	0	32	-43	-41

Table 3

Transmission Loss Through 1.5-In. i.d. Pipe Filled With Methanol

Frequency (GHz)	Reference free space	Coupling loss	Theoretical attenuation	Computed measurement	Actual measurement
4.0	7	20	65	-78	-83
4.5	7	19	67	-79	-87
5.0	7	18	65	-76	-81

Table 4

Transmission Loss Through 1.5-In. i.d. Pipe Filled With Distilled Water

Frequency (GHz)	Reference free space	Coupling loss	Theoretical attenuation	Computed measurement	Actual measurement
2.5	-5	24	47	-76	-74
3.0	13	22	58	-67	-72
3.5	11	21	68	-78	-79
4.0	7	20	67	-80	-77
4.5	7	19	66	-78	-84
5.0	7	18	59	-70	-82
5.5	2	14	54	-66	-85
6.0	12	24	53	-65	-79
6.5	-7	11	52	-70	-84

The theoretical attenuation in the pipe was found using program Pipe 1B. Because of the lack of published data on relative dielectric constants and loss tangents, these parameters were measured using a dielectric slab technique. Appendix D describes this technique and lists the values of the relative dielectric constants and loss tangents used in computing the waveguide attenuation.

The predicted measurement is equal to the free-space reference minus the sum of the coupling loss and theoretical waveguide attenuation (i.e., column 5 = column 2 - [column 3 + column 4] in Tables 2 through 4). The last column contains the actual measurement.

For carbon tetrachloride, the agreement between predicted and actual measurements is fairly good above cutoff. Below cutoff, the error is extremely large. No reason for this disagreement is known.

For methanol and distilled water, the actual measurement is consistently less than the predicted measurement (except in two cases). This can be explained by the reflection and refraction of the electromagnetic wave at the air-fluid interface. Electromagnetic waves undergo reflection and refraction at interfaces where the relative dielectric constants change. The reflection coefficient, R, is given by:

$$R = \frac{\sqrt{\epsilon}_1 - \sqrt{\epsilon}_2}{\sqrt{\epsilon}_1 + \sqrt{\epsilon}_2} \qquad \text{[Eq 1]}$$

where ϵ_1 is the relative dielectric constant of the first medium and ϵ_2 is the relative dielectric constant of the second medium. Therefore, the greater the mismatch of relative dielectric constants, the greater the reflection at the interface. This means there will be an additional power loss due to reflection and thus, a lower value of transmitted power.

Shielding Tests for Circular Waveguides

It is important to consider the accuracy of standard shielded enclosure test procedures in measuring the shielding effectiveness of enclosures with pipe penetrations. The cutoff frequency of a pipe is inversely proportional to the pipe radius and to the square root of the relative dielectric constant of the fluid in the pipe (i.e., as r or $\sqrt{\epsilon}$ increases, the cutoff frequency decreases). Neither MIL-STD-285 nor IEEE 299 make any statement about the contents of the penetrating pipe while it is being tested. Since any fluid besides air in the pipe will lower the cutoff frequency, it is important to have the pipe filled as it would be under normal use. Since the greatest amount of electromagnetic energy is coupled into the pipe when the plane wave is axially incident, the shielding effectiveness measurements should be taken with the transmitting and receiving antennas positioned along the pipe axis.

3 RESULTS

This chapter presents a series of graphs produced from FORTRAN Program Pipe 1B to be used in designing pipe penetrations for shielded enclosures. Before presenting these graphs, a few comments will be made about the effect of material parameters on waveguide attenuation and cutoff frequency.

Effect of Material Parameters on Attenuation

The loss tangent of the dielectric affects attenuation whereas the relative dielectric constant affects cutoff frequency. By definition, the cutoff frequency affects the attenuation. Figure 4 gives the attenuation of the lowest order mode (TE_{11}) of a 6-in. (15.24-cm) length of 1.475-in. (3.746-cm) i.d. pipe for distilled water at various loss tangents. The loss tangent and the relative dielectric constant are held constant throughout the frequency band. The value of the relative dielectric constant is 68.11. The loss tangent is stepped from 0.0 to 0.50 in 0.05 increments. The major effect of the loss tangent is to increase the attenuation. Note that a small change in the loss tangent can change the attenuation considerably, especially at frequencies well above cutoff.

Curves showing the change in cutoff frequency of the lowest order mode with relative dielectric constant are given in Figure 5. The curves represent pipe i.d. of 1.0 in. (2.54 cm), 1.5 in. (3.81 cm), 2.0 in. (5.08 cm), 2.5 in. (6.35 cm), 4.0 in. (10.16 cm), and 6.0 in. (15.24 cm). The relative dielectric constants range from 1 to 100. Note the steepness of each curve for low relative dielectric constants. This is caused by the inverse square root dependence of cutoff frequency on the relative dielectric constant.

Design Curves

Figures 6 through 14 give the attenuation of the lowest order mode (TE_{11}) in a 6-in. (15.24-cm) length of pipe for various fluids and pipe i.d. values. Each figure consists of six curves corresponding to i.d. values of 1.0 in. (2.54 cm), 1.5 in. (3.81 cm), 2.0 in. (5.08), 2.5 in. (6.35 cm), 4.0 in. (10.16 cm), and 6.0 in. (15.24 cm). The relative dielectric constants and loss tangents were taken from von Hippel[3] and are summarized in Table 5. For intermediate frequencies, a linear interpolation was performed on the given values. Because attenuation is directly proportional to length, to find the attenuation from a pipe of length L, the attenuation should be multiplied by L/6 (L in in.).

A few liquids have large changes in relative dielectric constant and loss tangent over the 100-MHz to 10-GHz range (e.g., methanol, ethylene glycol, and water). This might present problems in determining the optimal pipe size, especially since a small change in loss tangent can result in a large change in attenuation (see Figure 4).

[3]A. R. von Hippel, Dielectric Materials and Applications (Technology Press of the Massachusetts Institute for Technology, 1954).

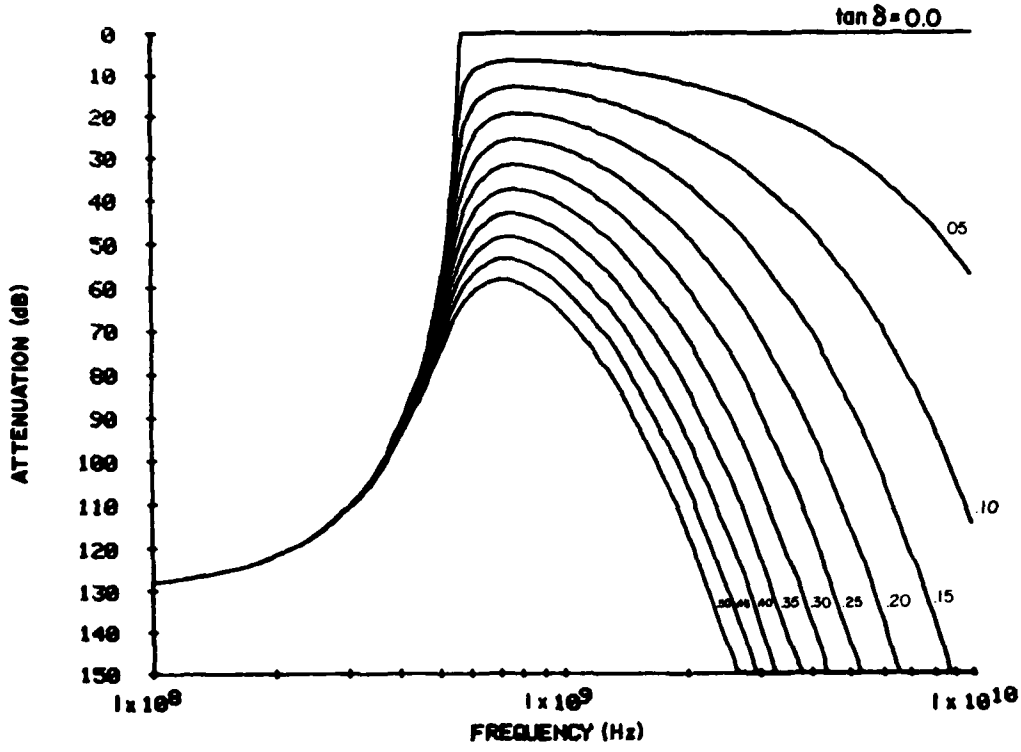

Figure 4. Theoretical attenuation of the TE_{11} mode for a 6-in. (15.2 cm) length of 1.5-in. (3.8-cm) i.d. pipe filled with distilled water for various loss tangents.

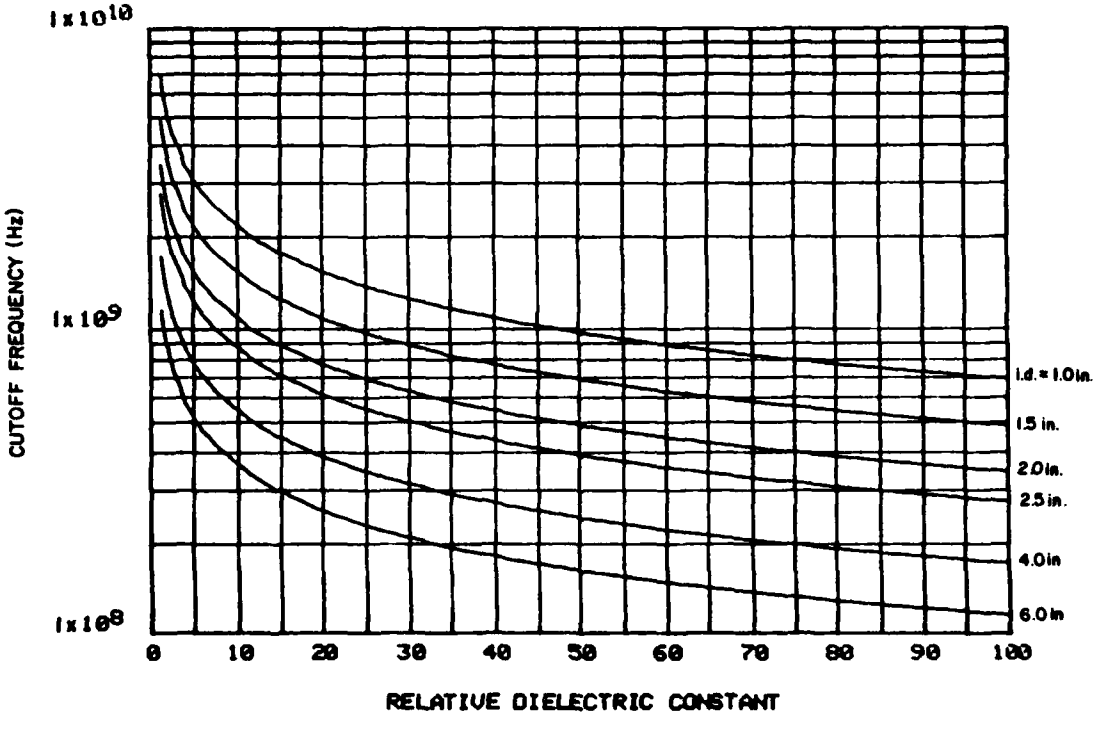

Figure 5. Cutoff frequency versus relative dielectric constant for various pipe diameters.

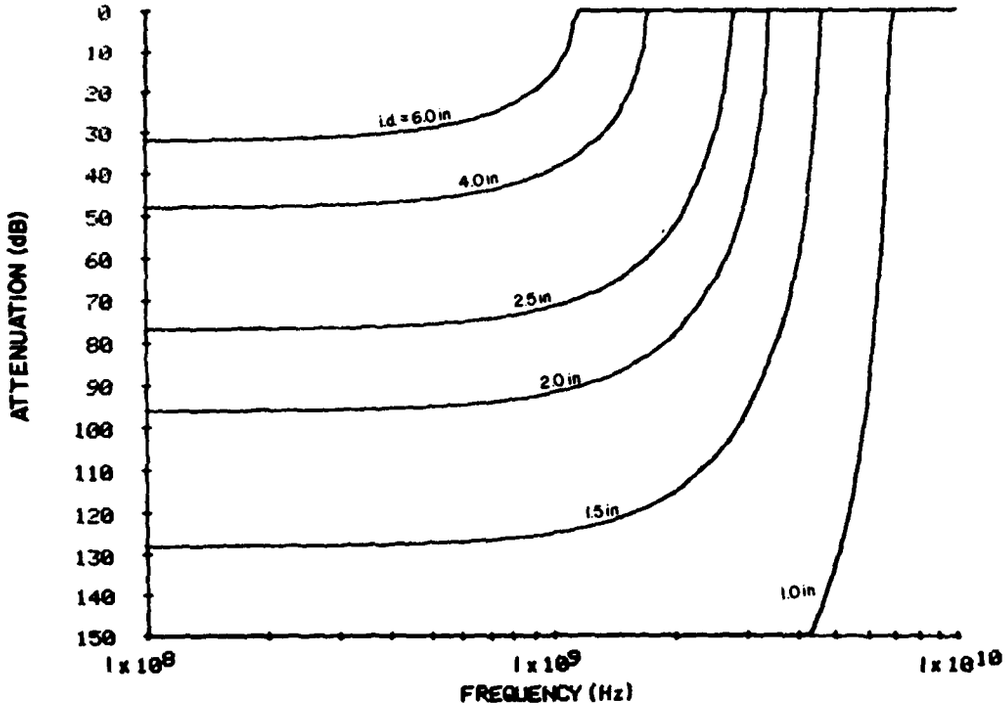

Figure 6. Theoretical attenuation of a 6-in. (15.2-cm) air-filled pipe (ε_r = 1) for various inside diameters.

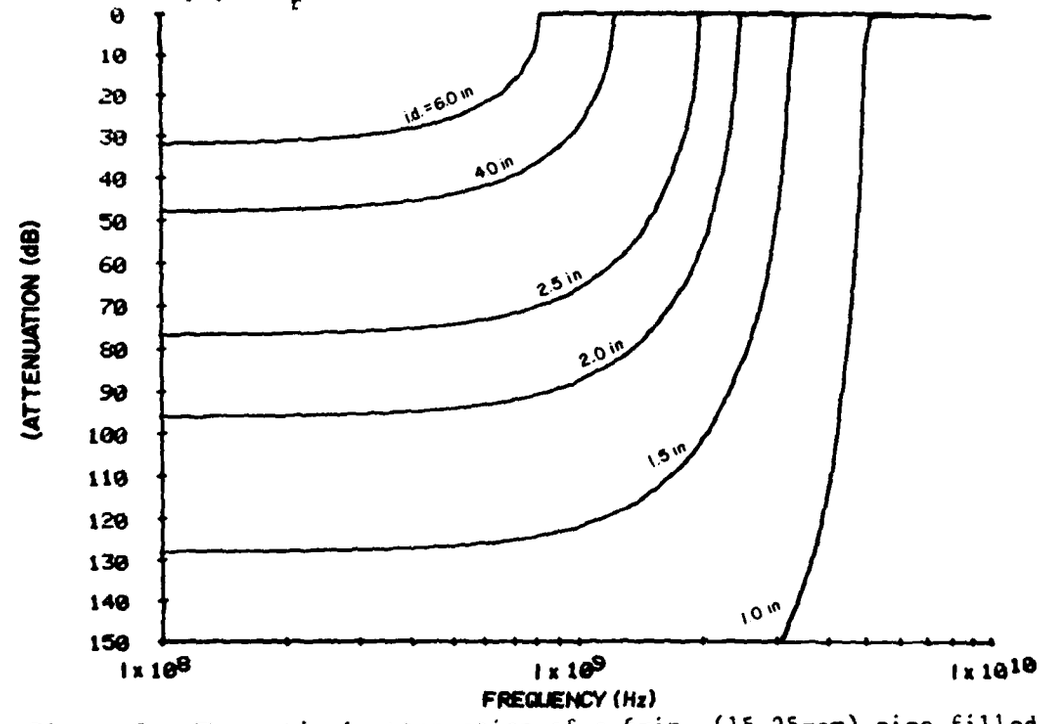

Figure 7. Theoretical attenuation of a 6-in. (15.25-cm) pipe filled with aviation gasoline (100 octane) (ε_r = 2) for various inside diameters.

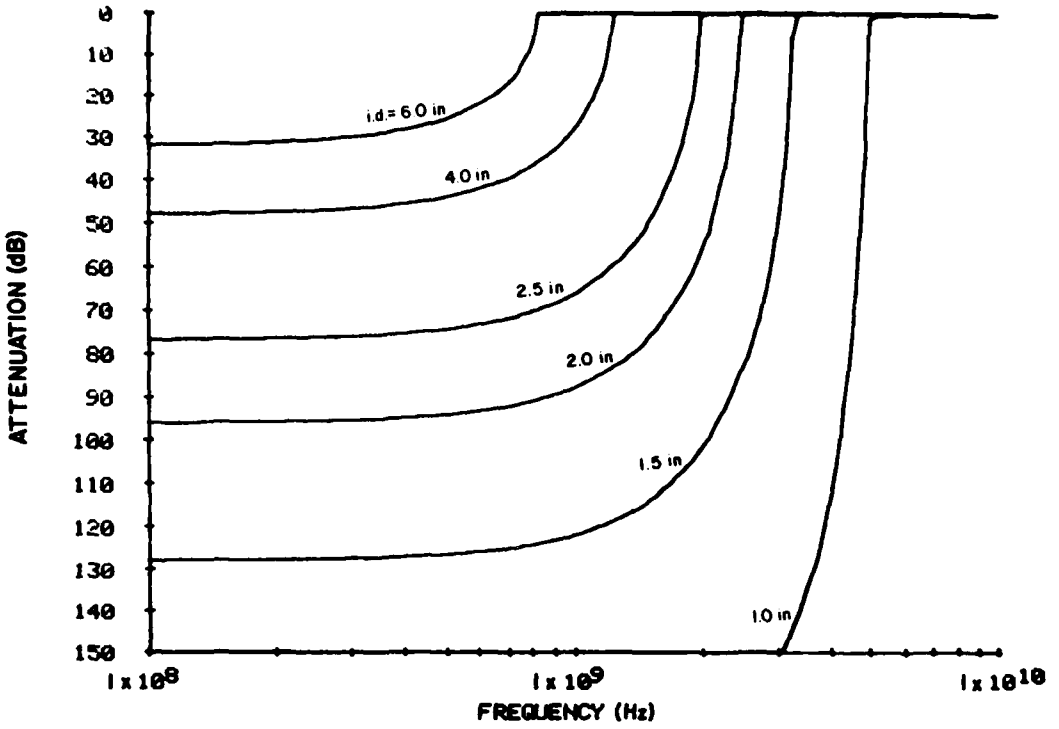

Figure 8. Theoretical attenuation of a 6-in. (15.25-cm) pipe filled with aviation gasoline (91 octane) ($\varepsilon_r \approx 2$) for various inside diameters.

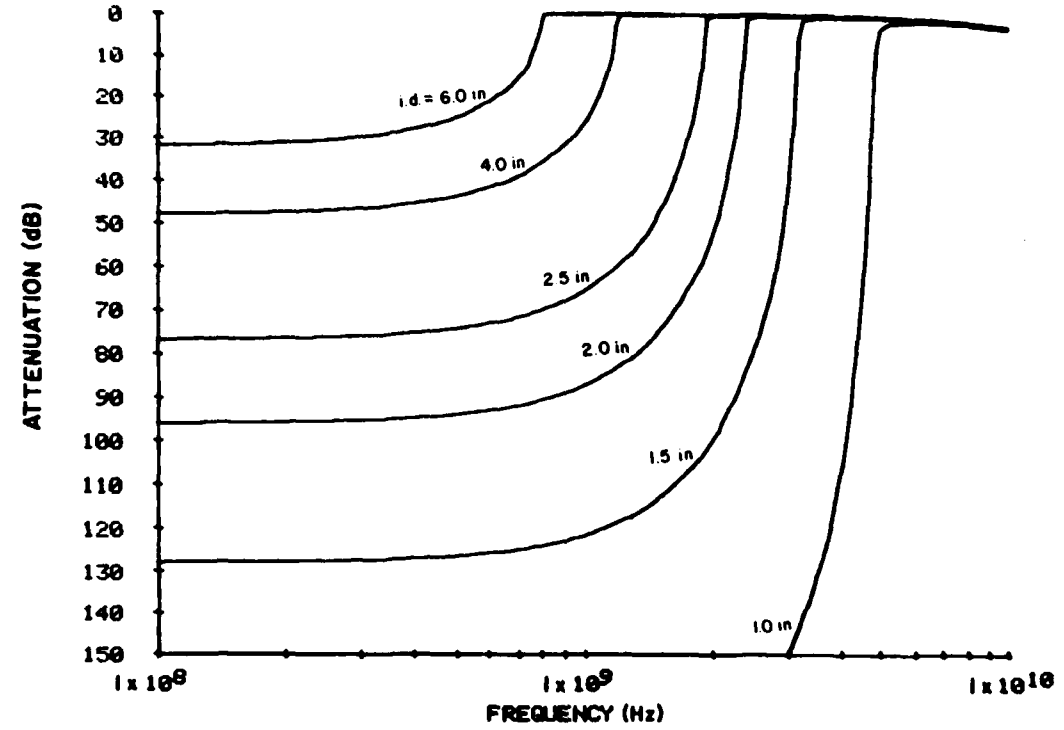

Figure 9. Theoretical attenuation of a 6-in. (15.25-cm) pipe filled with jet fuel (JP-3) ($\varepsilon_r \approx 2$) for various inside diameters.

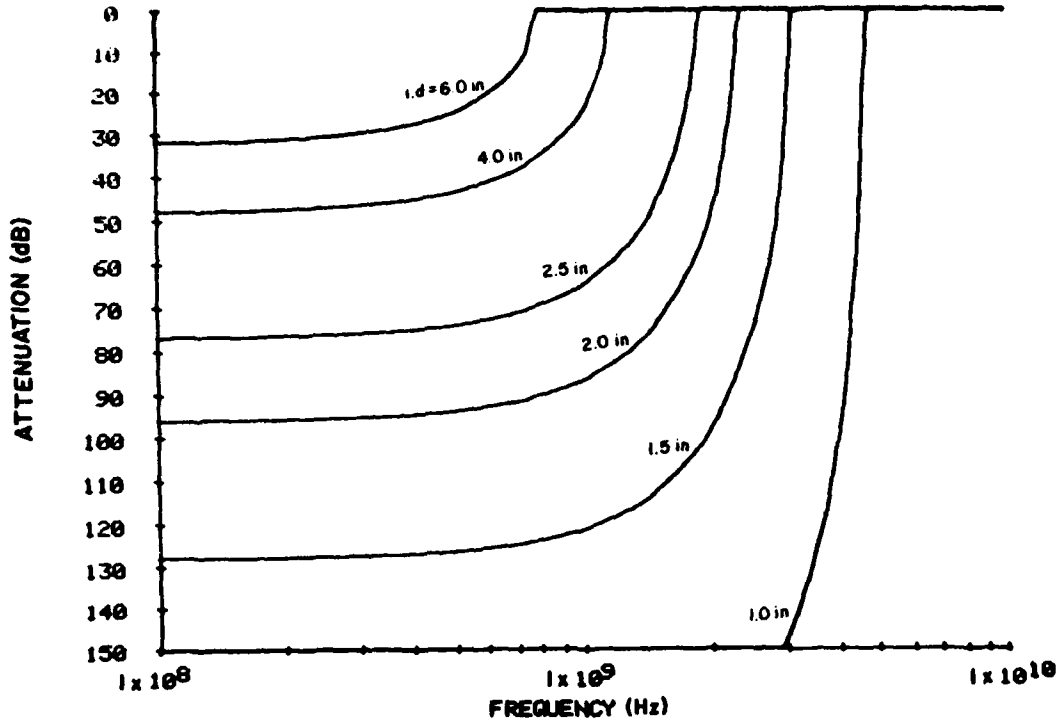

Figure 10. Theoretical attenuation of a 6-in. (15.25-cm) pipe filled with carbon tetrachloride ($\varepsilon_r \approx 2$) for various inside diameters.

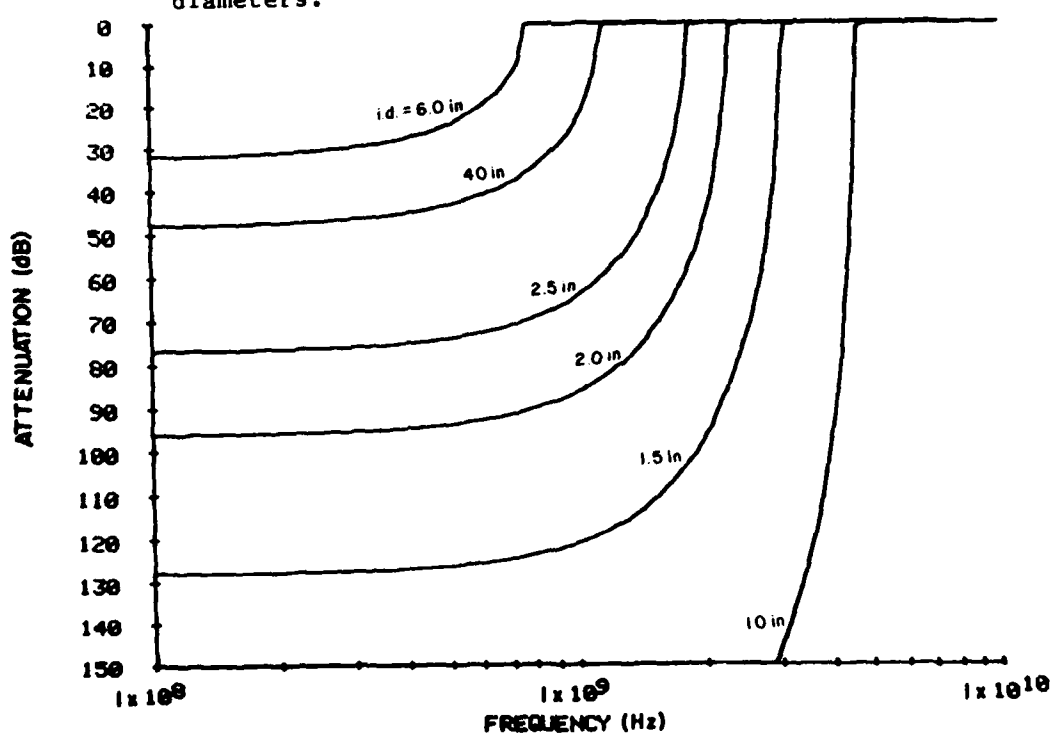

Figure 11. Theoretical attenuation of a 6-in. (15.25-cm) pipe filled with cable oil ($\varepsilon_r \approx 2$) for various inside diameters.

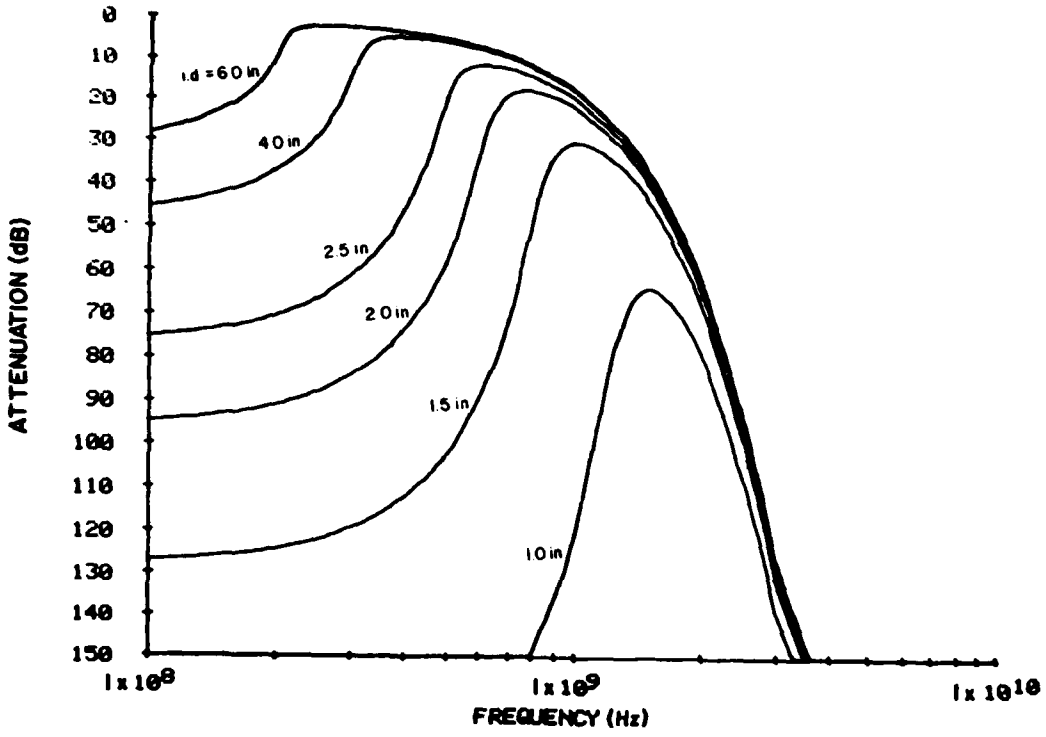

Figure 12. Theoretical attenuation of a 6-in. (15.25-cm) pipe filled with methanol ($\epsilon_r \approx 24$) for various inside diameters.

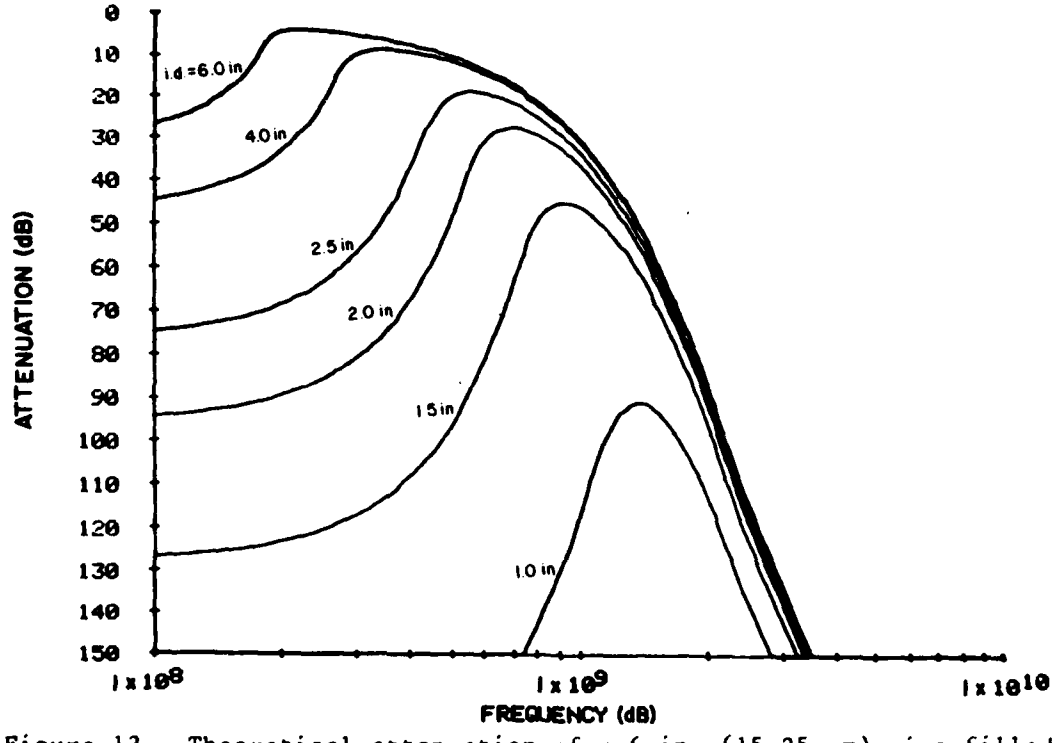

Figure 13. Theoretical attenuation of a 6-in. (15.25-cm) pipe filled with ethylene glycol ($\epsilon_r \approx 25$) for various inside diameters.

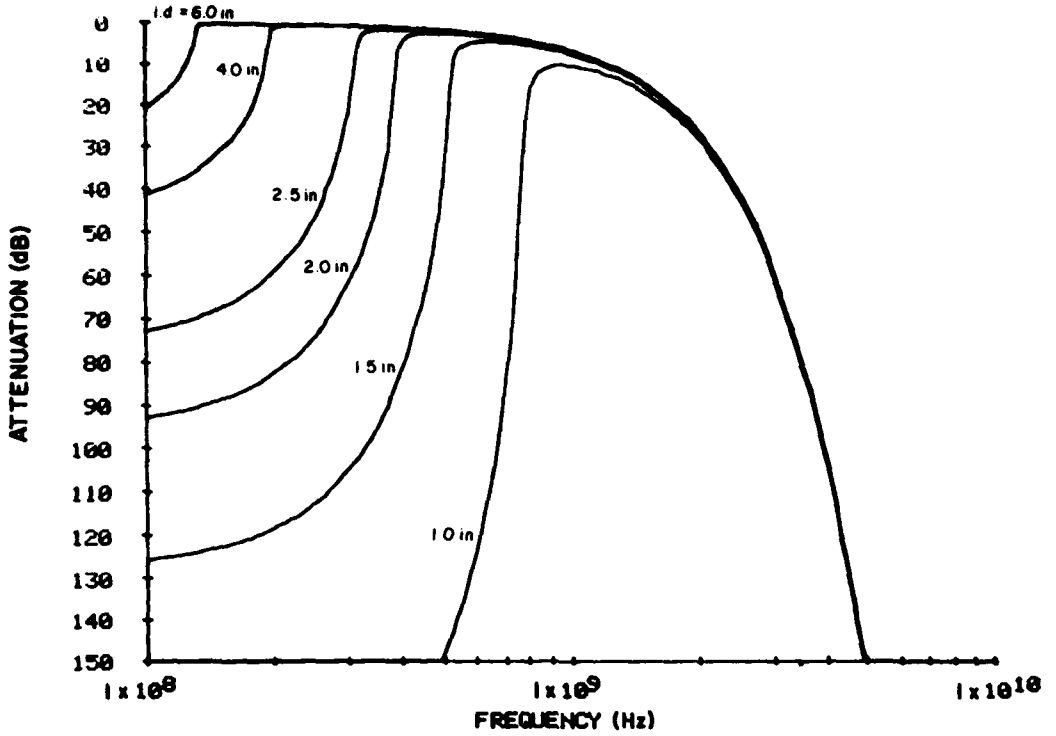

Figure 14. Theoretical attenuation of a 6-in. (15.25-cm) pipe filled with distilled water ($\varepsilon_r \approx 63$) for various inside diameters.

A worst-case analysis could be used in these cases. For example, a worst-case condition could assume a loss tangent of zero and a large relative dielectric constant (i.e., one greater than or equal to the maximum possible relative dielectric constant). However, this could lead to problems in practice. In designing a pipe penetration to carry distilled water, for example, assuming a relative dielectric constant of 80, the maximum cutoff frequency (from Figure 5) is approximately 750 MHz for a 1.0-in. (2.54-cm) i.d. pipe. With a loss tangent of zero, little attenuation will be expected above cutoff. To raise the cutoff frequency, either a smaller diameter pipe is needed or a honeycomb grating can be placed in the pipe (Appendix E). Either method will cause a reduction in the flow rate of the fluid in the pipe. The other alternative is to assume some loss tangent; then even at cutoff some attenuation will be present. For the values of Table 5, Figure 14 indicates an attenuation of approximately 10 dB at cutoff for the 1-in. (2.54-cm) i.d. pipe. Therefore, to obtain 70 dB of attenuation, a pipe of length L, with L given by

$$\frac{70 \text{ dB}}{10 \text{ dB}} = \frac{L}{6 \text{ in.}}$$

would be required. In this case, L = 42 in. -- a large length for a pipe penetration.

This calculation is based on values interpolated from from the data in Table 5. If the loss tangent and relative dielectric constant were known in greater detail, at smaller frequency increments, perhaps a more practical design could be achieved.

Table 5

Relative Dielectric Constants and Loss Tangents for Various Materials*

Frequency (MHz)	Relative dielectric constant (ε_r)	Loss tangent (tan δ)
Air		
100	1	0
1000	1	0
10000	1	0
Aviation gasoline - 100 Octane		
300	1.94	.00008
3000	1.92	.0014
Aviation gasoline - 91 Octane		
300	1.95	.00004
3000	1.94	.0015
Jet fuel - JP-3		
300	2.08	.0007
3000	2.04	.0055
Carbon tetrachloride		
100	2.17	<.0002
300	2.17	<.0001
3000	2.17	.0004
10000	2.17	.0016
Cable oil - Type 5314 (GE)		
300	2.24	.0039
3000	2.22	.0018
10000	2.22	.0022
Methanol at 25°C		
100	31.0	.038
300	30.9	.080
3000	23.9	.640
10000	8.9	.810
Ethlyene Glycol at 25°C		
100	41	.045
300	39	.160
3000	12	1.000
10000	7	.780
Distilled water at 25°C		
300	77.5	.016
3000	76.7	.157
10000	55.0	.540

*From A. R. von Hippel. These data were used to plot the curves shown in Figures 6 through 14.

4 CONCLUSIONS

This report has addressed the electromagnetic shielding effectiveness of waveguide sections (pipes) filled with fluids. An analytical method for determining the coupling between horn antennas when used to measure shielding effectiveness of shields with pipe penetrations has been presented. Analytical methods including computer codes for calculating attenuation versus frequency within the pipe sections have been developed and verified experimentally. From these analytical methods, design curves have been produced for commonly used pipe sizes and fluids. Similarly, analytical methods have been developed for honeycomb filters and calculations have been made to show shielding effectiveness of this filter versus frequency. Results show that:

1. For fluids with relatively high dielectric constants and low loss tangents, currently used designs can compromise the effectiveness of the shield.

2. A honeycomb grating can have its shielding effectiveness substantially reduced if filled with distilled water instead of air.

A problem encountered in this study is that published data on the relative dielectric constant and loss tangent are incomplete for most fluids of interest.

APPENDIX A:

WAVE PROPAGATION IN CIRCULAR METALLIC WAVEGUIDES

The analysis of circular metallic waveguides can be found in many standard electromagnetic textbooks.[4] Significant results are summarized here.

A circular metallic pipe supports both TE and TM waveguide modes. The propagation constants of these modes are given by:

$$\beta_{n,m} = \sqrt{\varepsilon_r}\, k_o \sqrt{1 - \left(\frac{f_{c(n,m)}}{f}\right)^2} \qquad \text{[Eq A1]}$$

where ε_r = relative dielectric constant of the medium filling the waveguide

k_o = free space wave number

$f_{c(n,m)}$ = cutoff frequency of the $TE_{n,m}$ or $TM_{n,m}$ mode

f = frequency of operation.

Equation A1 is valid for $f > f_{c(n,m)}$. For TE modes, the cutoff frequency is given by:

$$f_{c(n,m)} = \frac{1}{2\pi} \frac{\rho'_{n,m}}{a} \frac{c}{\sqrt{\varepsilon_r}} \qquad \text{[Eq A2]}$$

where a = radius of the waveguide

c = speed of light in free space

$\rho'_{n,m}$ = the mth root of J_n', the first derivative of the nth order Bessel function

Similarly, for TM modes:

$$f_{c(n,m)} = \frac{1}{2\pi} \frac{\rho_{n,m}}{a} \frac{c}{\sqrt{\varepsilon_r}} \qquad \text{[Eq A3]}$$

where $\rho_{n,m}$ = the mth root of J_n, the nth order Bessel function.

The $\rho_{n,m}$ and $\rho'_{n,m}$ values can be found in standard mathematical tables.[5] Tables A1 and A2 list values of $\rho'_{n,m}$ for m = 1, 2, 3 and n = 0, 1, 2, 3.

---

[4] S. Ramo, J. Whinnery, and T. Van Duzer, Field and Waves in Communication Electronics (John Wiley and Sons, Inc., 1965); R. E. Collin, Field Theory of Guided Waves (McGraw-Hill, Co., 1960).

[5] M. Abramovitz and I. Stegun, Handbook of Mathematical Functions (Dover Press, 1970).

Table A1

Roots of J_n', Derivative of the nth Order Bessel Function

m	n = 0	1	2	3
1	3.832	1.841	3.054	4.201
2	7.016	5.331	6.706	8.015
3	10.173	8.536	9.969	11.346

Table A2

Roots of J_n, nth Order Bessel Function

m	n = 0	1	2	3
1	2.405	3.832	5.136	6.380
2	5.520	7.016	8.417	9.761
3	8.654	10.173	11.620	13.015

For $f < f_{c(n,m)}$, the (n,m) waveguide mode is "cutoff." The attenuation constant is given by:

$$\alpha_{n,m} = \sqrt{\varepsilon_r}\, k_o \sqrt{\left(\frac{f_{c(n,m)}}{f}\right)^2 - 1} \qquad \text{[Eq A4]}$$

where ε_r, k_o, $f_{c(n,m)}$ and f are as defined in Equation A1.

These results, typically derived for the case in which the waveguide is filled with a lossless medium, are readily extended to the lossy case by allowing ε_r to be complex. Denoting the complex dielectric constant by ε_r^*,

$$\varepsilon_r^* = \varepsilon_r - i\frac{\sigma}{\omega\varepsilon_o} \qquad \text{[Eq A5]}$$

where ε_r = real relative dielectric constant

σ = conductivity of the medium

ε_o = free-space permittivity

$\omega = 2\pi f$.

A more convenient version of Equation A5 is:

$$\varepsilon_r^* = \varepsilon_r (1 - j\tan\delta) \qquad \text{[Eq A6]}$$

where $\tan \delta = \frac{\sigma}{\omega \varepsilon_o \varepsilon_r}$.

Tan δ is known as the loss tangent or dissipation factor. The loss tangent is a measure of a material's loss properties.

Substituting ε_r^* for ε_r in Equation A1 yields an expression for the complex propagation constant $\beta - j\alpha$. The branches of the complex square root are chosen such that α and β are positive real. That is, the solution corresponds to a forward propagating wave with attenuation.

It is important to note that there is no real cutoff frequency in a lossy waveguide. Equation A1 has a complex solution for all frequencies, rather than the purely real or purely imaginary solutions present in the lossless case. The cutoff frequency in the lossy case can still be defined as that for the lossless case. This definition is useful because as the frequency changes from $f > f_{c_{lossless}}$ to $f < f_{c_{lossless}}$, the wave shifts from one dominated by the propagation term, β, to one dominated by the attenuation term, α.

APPENDIX B:

COUPLING OF ELECTROMAGNETIC WAVES TO A CIRCULAR WAVEGUIDE

When an electromagnetic wave is incident on the open end of a circular waveguide, some of the wave's energy will be coupled into the waveguide. Analysis of the coupling factor is complicated by diffraction of the incident wave by the waveguide end. Pearson has determined theoretically the fields within the waveguide for a plane harmonic electromagnetic wave incident on a semi-infinite open-ended perfectly conducting circular waveguide.[6] This problem has been addressed experimentally by Southworth and King.[7] Experiments were done to determine the directive properties of metal pipes and horns when used as electromagnetic wave receivers. This appendix presents the basic textbook approach to power transfer between transmitter and receiver.[8]

Two important antenna parameters are directivity and effective aperture. The directivity of an antenna is a measure of the relative concentration of radiated or received power in different directions. It is dependent on antenna type and size.

Effective aperture is defined as the ratio of the power in the antenna terminating impedance to the power density of the incident wave. Under conditions of maximum power transfer and zero antenna losses, the effective aperture is a maximum. Maximum effective aperture is related to directivity through the expression:

$$D = \frac{4\pi}{\lambda^2} A_{em} \qquad \text{[Eq B1]}$$

where D is the directivity, A_{em} is the maximum effective aperature and λ is the wavelength.

Consider a transmitting antenna with directivity D_T and a receiving antenna with maximum effective aperture A_{eR} (Figure B1). The antennas are separated by a distance d. The received power, P_R, is given by:

$$P_R = P_T D_T \left[\frac{1}{4\pi d^2}\right] A_{eR} \qquad \text{[Eq B2]}$$

---

[6] J. D. Pearson, "The Diffraction of Electro-Magnetic Waves by a Semi-Infinite Circular Wave Guide," Proceedings of the Cambridge Philosophical Society, Vol 49, Part 4 (1953), pp 659-667.

[7] G. C. Southworth, and A. P. King, "Metal Horns as Directive Receivers of Ultra-Short Waves," Proceedings of the I.R.E., Vol 27 (February 1939), pp 95-102.

[8] J. D. Kraus, Antennas (McGraw-Hill, Co., 1950); R. E. Collin and F. J. Zucker, Antenna Theory, Part 1 (McGraw-Hill, 1969).

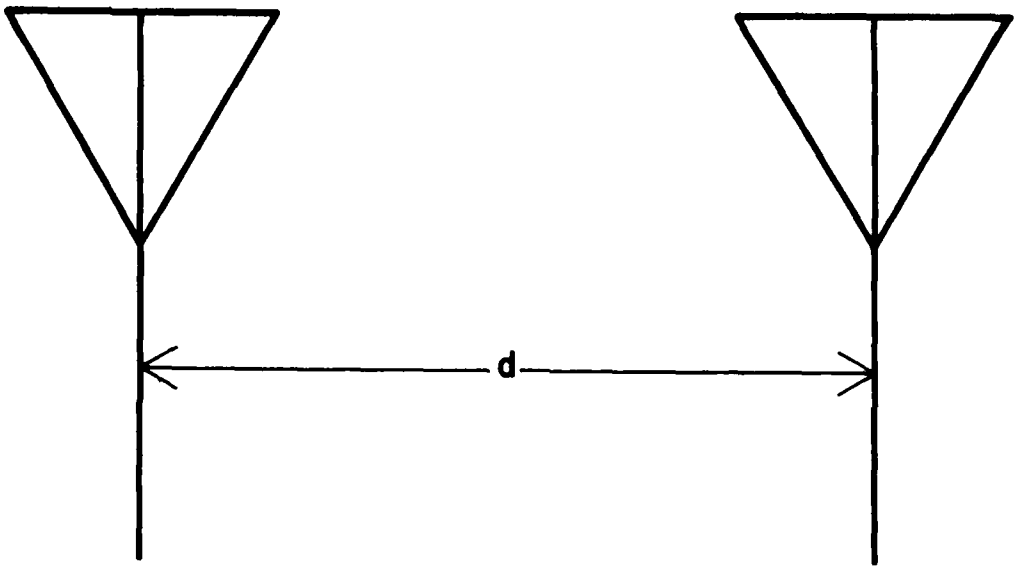

Figure B1. Transmitting and receiving antennas.

where P_T is the transmitted power. This formula assumes a lossless medium and no polarization mismatch. Using Equation B1, Equation B2 can be expressed in terms of the directivity of the receiving antenna, D_R:

$$P_R = D_T D_R \left[\frac{\lambda}{4\pi d}\right]^2 P_T \qquad \text{[Eq B3]}$$

Therefore, the power transfer ratio between two antennas is:

$$\frac{P_R}{P_T} = D_T D_R \left[\frac{\lambda}{4\pi d}\right]^2 \qquad \text{[Eq B4]}$$

Equation B4 is a far-field relation and, therefore, will not be valid if d is small compared to the size of the antenna. The error is small if:

$$d \geq \frac{2l^2}{\lambda} \qquad \text{[Eq B5]}$$

where l is the maximum linear dimension of either antenna.

The directivity of a horn antenna with a large aperture can be written in terms of the maximum effective aperture. Thus, from Equation B1:

$$D = \gamma 4\pi A_{E\lambda} A_{H\lambda} \qquad \text{[Eq B6]}$$

where $A_{E\lambda}$ = aperture length in free-space wavelengths in E plane

$A_{H\lambda}$ = aperture length in free-space wavelengths in H plane

γ = ratio of maximum effective aperture to physical aperture.

An optimum horn has a value of $\gamma \approx 0.6$. Thus, Equation B6 becomes:

$$D \approx 7.5\ A_{E\lambda}\ A_{H\lambda} \qquad \text{[Eq B7]}$$

The horns used in the tests conducted for this report have an aperture size of 5.85 in. (14.86 cm) (E-plane) by 7.92 in. (20.12 cm) (H-plane). So,

$$A_{E\lambda} = \frac{14.86\ \text{cm}}{\lambda}$$

$$A_{H\lambda} = \frac{20.12\ \text{cm}}{\lambda} \qquad \text{[Eq B8]}$$

Therefore, the directivity of the horn antennas, D_H, is given by

$$D_H \approx 7.5 \left[\frac{14.86}{\lambda} \cdot \frac{20.12}{\lambda} \right] = \frac{2242}{\lambda^2} \qquad \text{[Eq B9]}$$

where λ is measured in cm.

The open-ended waveguide can be considered as an antenna. The directivity of an open-ended circular waveguide is given by

$$D_P \approx 10.5\ \pi \frac{r^2}{\lambda^2} \qquad \text{[Eq B10]}$$

where r is the radius of the waveguide. The pipes (circular waveguides) used in the tests have radii of 0.738 in. (1.874 cm) and 2.0 in. (5.08 cm). Thus,

$$D_{P_S} \approx \frac{10.5\pi}{\lambda^2} (1.874)^2 = \frac{116}{\lambda^2} \qquad \text{[Eq B11]}$$

for the small pipe and

$$D_{P_L} \approx \frac{10.5\pi}{\lambda^2} (5.08)^2 = \frac{851}{\lambda^2} \qquad \text{[Eq B12]}$$

for the large pipe. Again, λ is measured in cm.

Figures B2 and B3 show the placement of the horn antennas used in these tests. Figure B2 shows the positioning in free space for the reference measurements. The distance d was measured from mouth to mouth. For testing the waveguide below cutoff theory, the configuration in Figure B3 was used.

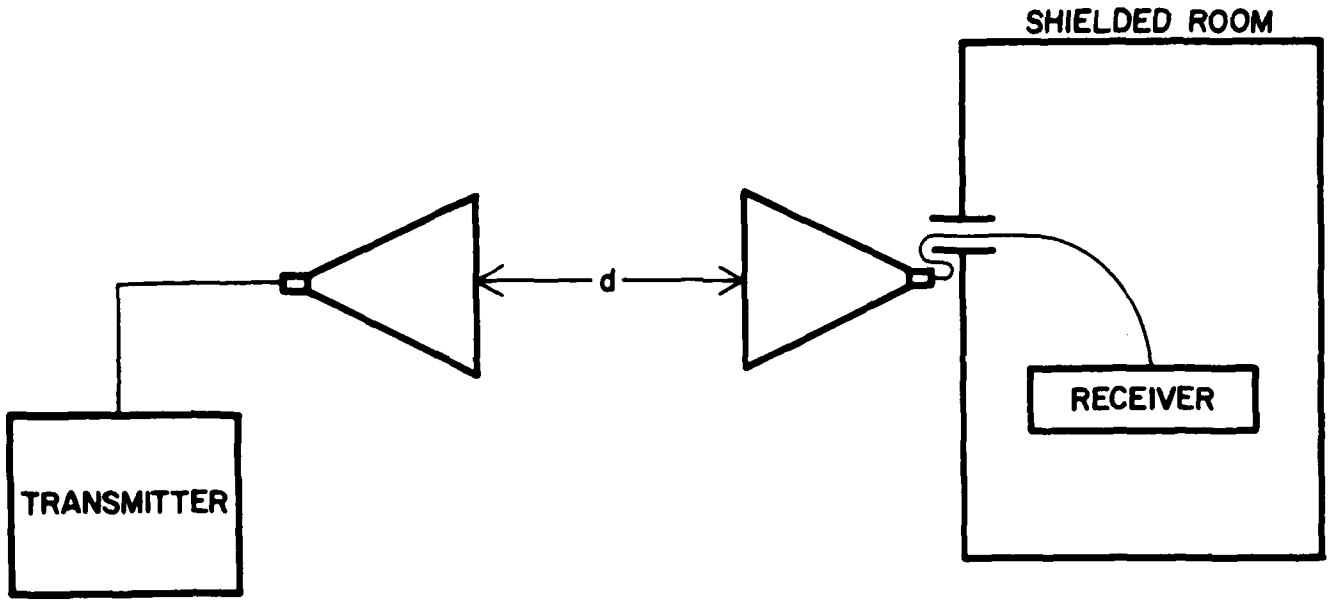

Figure B2. Experimental setup for reference measurements.

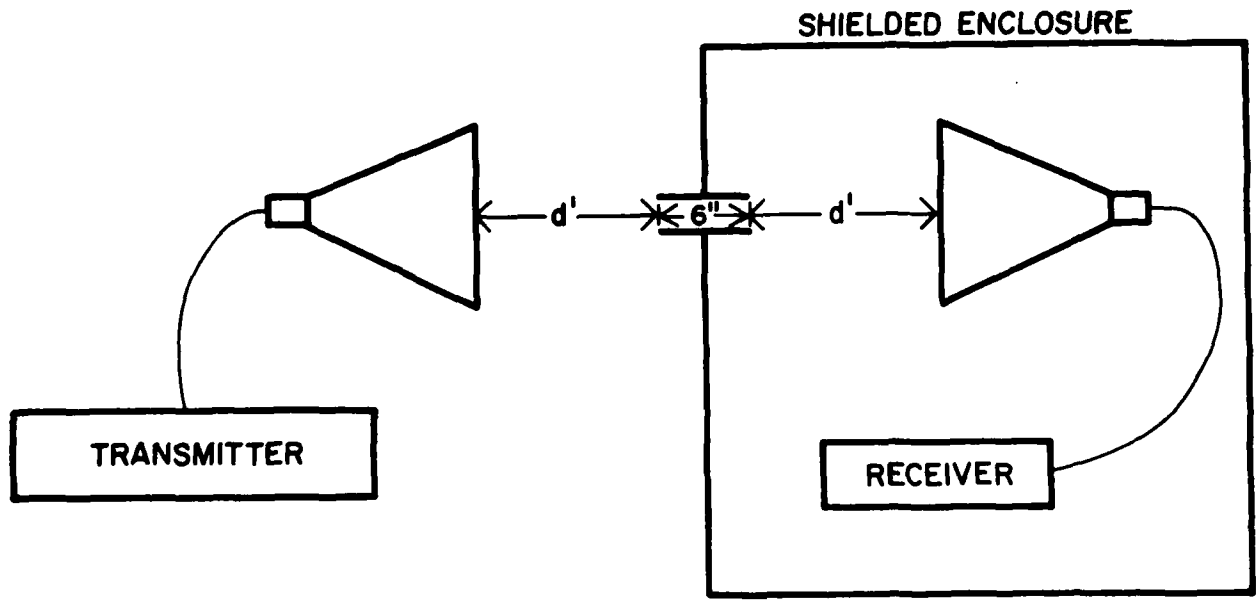

Figure B3. Experimental setup for waveguide measurements.

The waveguide was 6 in. (15.24 cm) long with a radius r, and d' is the distance from the horn mouth to the end of the waveguide.

As an example calculation for coupling loss, consider a plane wave at 2.5 GHz propagating from the transmitting antenna toward the large pipe. Some of the transmitted wave power will be coupled into the pipe and some will be diffracted, which results in a coupling loss. Some of the wave power that coupled into the pipe will retransmit at the other end of the pipe. Again, there will be a coupling loss. Finally, the resultant wave power will be sampled by the receiving horn.

The coupling loss is one-half the dB difference between horn-to-horn power transfer and horn-to-pipe-to-horn power transfer. If P_{H-H} denotes the power transfer ratio between the two horns in free space and P_{H-P-H} denotes the power transfer ratio between the two horns separated by the pipe, then coupling loss, L_C, s:

$$L_C = \frac{P_{H-H} - P_{H-P-H}}{2} \text{ (in dB)} \qquad \text{[Eq B13]}$$

Let the horn-to-horn distance d (Figure B2) be 78 in. (198 cm). Then:

$$P_{H-H} = \frac{P_R}{P_T} = D_T D_R \left[\frac{\lambda}{4\pi d}\right]^2$$

$$= D_H D_H \left[\frac{\lambda}{4\pi d}\right]^2 \qquad \text{[Eq B14]}$$

Using Equation B9:

$$P_{H-H} = \left[\frac{2242}{\lambda^2}\right]^2 \left[\frac{\lambda}{4\pi d}\right]^2 \qquad \text{[Eq B15]}$$

Recalling:

$$\lambda = \frac{c}{f} \frac{3 \times 10^{10}}{2.5 \times 10^{9}} = 12 \text{ cm} \qquad \text{[Eq B16]}$$

Thus,

$$P_{H-H} = \left[\frac{2242}{144}\right]^2 \left[\frac{12}{4\pi\ (198)}\right]^2 = .00564 \qquad \text{[Eq B17]}$$

Expressed in dB:

$$P_{H-H} = 10 \log_{10} (.00564) = -22.5 \qquad \text{[Eq B18]}$$

Let the horn-to-pipe distance d' (Figure B2b) be 36 in. (91.4 cm). Then:

$$P_{H-P_L} = D_H D_P \left[\frac{\lambda}{4\pi d'}\right]^2 \qquad \text{[Eq B19]}$$

Using Equations B9 and B12:

$$P_{H-P_L} = \left[\frac{2242}{\lambda^2}\right] \left[\frac{851}{\lambda^2}\right] \left[\frac{\lambda}{4\pi d'}\right]^2 \qquad \text{[Eq B20]}$$

Thus,

$$P_{H-P_L} = \left[\frac{2242}{144}\right] \left[\frac{851}{144}\right] \left[\frac{12}{4\pi\ (91.4)}\right]^2 = .01 \qquad \text{[Eq B21]}$$

Expressed in dB:

$$P_{H-P_L} = -20 \text{ dB} \qquad \text{[Eq B22]}$$

Because of reciprocity:

$$P_{H-P_L} = P_{P_L-H} \qquad \text{[Eq B23]}$$

So:

$$P_{H-P_L-H} = 2\ P_{H-P_L} = -40 \text{ dB} \qquad \text{[Eq B24]}$$

Therefore,

$$L_C = \frac{-22.5 - (-40)}{2} = 8.75 \text{ dB} \qquad \text{[Eq B25]}$$

With the transmitter supplying 5 W at 2.5 GHz, a value of +5 dBm was measured by the receiver for the reference measurement. The waveguide measurement was -10 dBm. This results in a measured coupling loss of:

$$L_C = \frac{+5 - (-10)}{2} = 7.5 \text{ dB} \qquad \text{[Eq B26]}$$

The error in reading the receiver is $\pm$1/2 dB, giving a $\pm$3/4 dB error in the measured coupling loss. Greater error probably exists in the reference measurement. Because of cable constraints (too short), it was not possible to move the receiving horn farther than 36 in. (91.4 cm) from the shielded enclosure. This put the receiving horn in the "standing wave" field between the enclosure and the transmitting horn, resulting in a non-free-field measurement for the reference reading.

APPENDIX C:

FORTRAN PROGRAMS TO CALCULATE WAVEGUIDE ATTENUATION
RESULTING FROM DIELECTRIC LOADING

Programs Pipe 1A and Pipe 1B (Figures C1 and C2) calculate the overall attenuation in dB of an electromagnetic wave propagating through a length of circular waveguide (pipe). Program Pipe 1A uses one relative dielectric constant and loss tangent to compute the attenuation for a band of frequencies. Program Pipe 1B uses a separate relative dielectric constant and loss tangent for each frequency.

The attenuation factor (in Np/cm) of a circular waveguide is the real part of the complex propagation constant,

$$\gamma = \sqrt{h^2_{nm} - \omega^2 \mu\varepsilon} \qquad \text{[Eq C1]}$$

where ω = angular frequency (rad/sec)

μ = permeability of the material in the waveguide

ε = permittivity of the material in the waveguide, and:

$$h_{nm} = \frac{(ha)_{nm}}{a} \qquad \text{[Eq C2]}$$

where a is the pipe radius and $(ha)_{nm}$ is the mth root of a Bessel function of the nth order. Values of $(ha)_{nm}$ for TM modes are given in Appendix A, Table A2; values of $(ha)_{nm}$ for TE modes are given in Table A1.

The cutoff frequency of the (n,m) mode is the frequency for which the real part of γ^2 is zero. Attenuation through the waveguide is a minimum at the cutoff frequency.

$$f_c = \frac{h_{nm}}{2\pi\sqrt{\mu\varepsilon}} \qquad \text{[Eq C3]}$$

Since

$$c = \frac{1}{\sqrt{\mu_o \varepsilon_o}} \qquad \text{[Eq C4]}$$

where c is the speed of light in a vacuum,

```
      PROGRAM PIPE1A(INPUT,TAPE6=INPUT)
C
C     A PROGRAM TO CALCULATE THE ATTENUATION IN A CIRCULAR METALLIC
C     WAVEGUIDE FILLED WITH LOSSY DIELECTRIC.
C
C     FEATURES:  WAVEGUIDE ATTENUATION CALCULATIONS
C                CALCULATIONS OVER A FREQUENCY RANGE
C
C-----------------------------------------------------------------------
C
C     ELECTROMAGNETIC COUPLING THROUGH A FLUID FILLED PIPE IS MODELLED
C     BY THE ATTENUATION IN THE TE(11) CIRCULAR WAVEGUIDE MODE.  THIS
C     REPRESENTS THE FOLLOWING TWO CASES.
C
C     1)  WORST-CASE ANALYSIS - ALL THE ELECTROMAGNETIC ENERGY
C         INCIDENT ON THE COUPLING REGION OF THE PIPE IS COUPLED INTO
C         THE LOWEST ORDER WAVEGUIDE MODE.
C
C     2)  ACCURATE KNOWLEDGE OF THE EXCITATION MECHANISM WHEREBY
C         ELECTROMAGNETIC ENERGY IS COUPLED INTO THE WAVEGUIDE IS
C         UNAVAILABLE, MAKING A MORE ACCURATE MODAL ANALYSIS
C         IMPOSSIBLE.
C-----------------------------------------------------------------------
C     USAGE:  COMPILE WITH THE FTN5 (FORTRAN 77) COMPILER.
C
C             THE PROGRAM IS WRITTEN TO BE USED INTERACTIVELY.  INPUT
C             IS ENTERED FROM THE TERMINAL IN RESPONSE TO QUESTIONS.
C             OUTPUT IS PRINTED TO THE TERMINAL.
C
C             FREQUENCY AND OVERALL ATTENUATION IS ALSO WRITTEN TO AN
C             OUTPUT FILE USING THE "*" FORMAT.  THIS FILE CAN THEN BE
C             PRINTED OR PLOTTED AT A LATER TIME.  THE USER IS
C             PROMPTED FOR AN OUTPUT FILE NAME.  A DEFAULT NAME
C             ("OUTPF") IS PROVIDED IF THE USER ENTERS A CARRIAGE
C             RETURN IN RESPONSE TO THIS QUESTION.  THE OUTPUT FILE IS
C             AUTOMATICALLY SAVED UNLESS THE DEFAULT NAME IS USED.
C             WHEN USING THE DEFAULT NAME, THE OUTPUT FILE REMAINS
C             LOCAL AND MUST BE EXPLICITLY SAVED (IF DESIRED) USING
C             SYSTEM LEVEL COMMANDS.
C
C     INPUT:  PIPE RADIUS IN CM
C             PIPE LENGTH IN CM
C             DIELECTRIC CONSTANT
C             LOSS TANGENT
C             MINIMUM FREQUENCY IN GHZ
```

Figure C1. Program Pipe 1A.

```
46 C                MAXIMUM FREQUENCY IN GHZ
47 C                FREQUENCY INCREMENT IN GHZ
48 C                OUTPUT FILE NAME
49 C
50 C        OUTPUT: ATTENUATION CONSTANT (ALPHA) IN NEPERS/CM
51 C                ATTENUATION CONSTANT (ALPHA) IN DB/CM
52 C                OVERALL ATTENUATION IN DB
53 C
54 C        OUTPUT TO FILE: FREQUENCY IN GHZ VS. OVERALL ATTENUATION IN DB
55 C
56 C                                        LANGUAGE:   FORTRAN 77
57 C                                        PROGRAMMER: SCOTT L. RAY
58 C                                        DATE:       7/11/83
59 C
60          COMPLEX GAMMA,J
61          REAL LENGTH,KO,KC
62          CHARACTER *7 NAME,NTEMP
63          PI=3.14159265
64          J=(0.0,1.0)
65          P11P=1.84118
66          A1=ALOG10(2.71828183)
67          PRINT 1000
68          READ *,RADIUS
69          KC=P11P/RADIUS
70          PRINT 1010
71          READ *,LENGTH
72          PRINT 1020
73          READ *,EPSR
74          FC=1.0/(2.0*PI)*(29.997925/SQRT(EPSR))*KC
75          PRINT 1030
76          READ *,DISP
77          PRINT 1040
78          READ *,FMIN
79          PRINT 1050
80          READ *,FMAX
81          PRINT 1060
82          READ *,FINC
83          NAME='OUTPF'
84          PRINT 1070
85          READ(6,2030,END=10) NTEMP
86          NAME=NTEMP
87 10       REWIND 6
88          OPEN(3,FILE=NAME)
89          PRINT 2060
90          PRINT 2040
```

Figure C1. (Cont'd).

```
 91          PRINT 1080,RADIUS,LENGTH
 92          PRINT 1090,EPSR,DISP
 93          PRINT 2000,FC
 94          PRINT 2010
 95          PRINT 2050
 96          DO 20 FREQ=FMIN,(FMAX+FINC/2.0),FINC
 97             KO=2.0*PI*FREQ/30.0
 98             GAMMA=CSQRT(KC*KC-EPSR*(1.0-J*DISP)*KO*KO)
 99             ALPHA=REAL(GAMMA)
100             ALPDB=20.0*A1*ALPHA
101             ATTEN=ALPDB*LENGTH
102             PRINT 2020,FREQ,ALPHA,ALPDB,ATTEN
103             WRITE(3,*) FREQ,ATTEN
104 20       CONTINUE
105          PRINT 2040
106          CLOSE(3)
107          IF(NAME.NE.'OUTPF') CALL PF('SAVE',NAME)
108          STOP
109 1000     FORMAT('ENTER PIPE RADIUS IN CM')
110 1010     FORMAT('ENTER PIPE LENGTH IN CM')
111 1020     FORMAT('ENTER DIELECTRIC CONSTANT')
112 1030     FORMAT('ENTER THE LOSS TANGENT')
113 1040     FORMAT('ENTER MINIMUM FREQUENCY IN GHZ')
114 1050     FORMAT('ENTER MAXIMUM FREQUENCY IN GHZ')
115 1060     FORMAT('ENTER FREQUENCY INCREMENT IN GHZ')
116 1070     FORMAT('ENTER THE OUPUT FILE NAME, (DEFAULT OUTPF)')
117 1080     FORMAT(/'RADIUS = ',F7.3,' CM',5X,'LENGTH = ',F8.3,' CM')
118 1090     FORMAT('EPSILON = ',F6.2,8X,'LOSS TANGENT = ',F6.4)
119 2000     FORMAT(/'  CUTOFF FREQUENCY = ',F7.3,' GHZ')
120 2010     FORMAT(/3X,'FREQ (GHZ)',3X,'ALPHA (NEPERS/CM)',3X,'ALPHA (DB/CM)
121       *',3X,'ATTEN (DB)')
122 2020     FORMAT(5X,F5.2,9X,1PE10.3,10X,0PF5.2,8X,F7.2)
123 2030     FORMAT(A7)
124 2040     FORMAT('-------------------------------------------------------
125       *------')
126 2050     FORMAT(3X,'-------------------------------------------------------
127       *------')
128 2060     FORMAT(//)
129          END
```

Figure C1. (Cont'd).

```
      PROGRAM PIPE1B(INPUT,TAPE6=INPUT)
C
C     A PROGRAM TO CALCULATE THE ATTENUATION IN A CIRCULAR METALLIC
C     WAVEGUIDE FILLED WITH LOSSY DIELECTRIC.
C
C     FEATURES:  WAVEGUIDE ATTENUATION CALCULATIONS
C                USER SPECIFIES EACH FREQUENCY
C                ABILITY TO CHANGE MATERIAL PARAMETERS AT EACH NEW
C                FREQUENCY
C
C ---------------------------------------------------------------------
C
C     ELECTROMAGNETIC COUPLING THROUGH A FLUID FILLED PIPE IS MODELLED
C     BY THE ATTENUATION IN THE TE(11) CIRCULAR WAVEGUIDE MODE.  THIS
C     REPRESENTS THE FOLLOWING TWO CASES.
C
C     1)  WORST-CASE ANALYSIS - ALL THE ELECTROMAGNETIC ENERGY
C         INCIDENT ON THE COUPLING REGION OF THE PIPE IS COUPLED INTO
C         THE LOWEST ORDER WAVEGUIDE MODE.
C
C     2)  ACCURATE KNOWLEDGE OF THE EXCITATION MECHANISM WHEREBY
C         ELECTROMAGNETIC ENERGY IS COUPLED INTO THE WAVEGUIDE IS
C         UNAVAILABLE, MAKING A MORE ACCURATE MODAL ANALYSIS
C         IMPOSSIBLE.
C ---------------------------------------------------------------------
C     USAGE:  COMPILE WITH THE FTN5 (FORTRAN 77) COMPILER.
C
C             THE PROGRAM IS WRITTEN TO BE USED INTERACTIVELY.  INPUT
C             IS ENTERED FROM THE TERMINAL IN RESPONSE TO QUESTIONS.
C             OUTPUT IS PRINTED TO THE TERMINAL.
C
C             WHEN CALCULATIONS ARE COMPLETED FOR ONE FREQUENCY AND
C             SET OF MATERIAL PARAMETERS, THE USER IS PROMPTED FOR
C             NEXT FREQUENCY, DIELECTRIC CONSTANT, AND LOSS TANGENT.
C             PREVIOUS VALUES ARE USED AS DEFAULTS.  A DEFAULT VALUE
C             IS OBTAINED BY HITTING CARRIAGE RETURN IN RESPONSE TO
C             THE PROMPTING QUESTION.
C
C             FREQUENCY AND OVERALL ATTENUATION ARE WRITTEN TO AN
C             OUTPUT FILE USING THE "*" FORMAT.  THIS FILE CAN THEN BE
C             PRINTED OR PLOTTED AT A LATER TIME.  THE USER IS
C             PROMPTED FOR AN OUTPUT FILE NAME.  A DEFAULT NAME
C             ("OUTPF") IS PROVIDED IF THE USER ENTERS A CARRIAGE
C             RETURN IN RESPONSE TO THIS QUESTION.  THE OUTPUT FILE IS
C             AUTOMATICALLY SAVED UNLESS THE DEFAULT NAME IS USED.
```

Figure C2. Program Pipe 1B.

```
46 C               WHEN USING THE DEFAULT NAME, THE OUTPUT FILE REMAINS
47 C               LOCAL AND MUST BE EXPLICITLY SAVED (IF DESIRED) USING
48 C               SYSTEM LEVEL COMMANDS.
49 C
50 C       INPUT:  PIPE RADIUS IN CM
51 C               PIPE LENGTH IN CM
52 C               DIELECTRIC CONSTANT
53 C               LOSS TANGENT
54 C               FREQUENCY IN GHZ
55 C               OUTPUT FILE NAME
56 C
57 C       OUTPUT: ATTENUATION CONSTANT (ALPHA) IN NEPERS/CM
58 C               ATTENUATION CONSTANT (ALPHA) IN DB/CM
59 C               OVERALL ATTENUATION IN DB
60 C
61 C       OUTPUT TO FILE: FREQUENCY IN GHZ VS. OVERALL ATTENUATION IN DB
62 C
63 C                                          LANGUAGE:   FORTRAN 77
64 C                                          PROGRAMMER: SCOTT L. RAY
65 C                                          DATE:       7/11/83
66 C
67          REAL LENGTH,KO,KC
68          COMPLEX J,GAMMA
69          CHARACTER *7 NAME,NTEMP
70          PI=3.14159265
71          J=(0.0,1.0)
72          P11P=1.84118
73          A1=ALOG10(2.71828183)
74          EPSR=1.0
75          DISP=0.0
76          PRINT 1000
77          READ *,RADIUS
78          KC=P11P/RADIUS
79          PRINT 1010
80          READ *,LENGTH
81          NAME='OUTPF'
82          PRINT 1020
83          READ(6,2010,END=10) NTEMP
84          NAME=NTEMP
85 10       REWIND 6
86          OPEN(3,FILE=NAME)
87          PRINT 2020
88          PRINT 1030
89          READ *,FREQ
90 20       REWIND 6
```

Figure C2. (Cont'd).

```
 91          KO=2.0*PI*FREQ/30.0
 92          PRINT 1040,EPSR
 93          READ(6,*,END=30)TEMP
 94          EPSR=TEMP
 95 30       REWIND 6
 96          FC=1.0/(2.0*PI)*(29.997925/SQRT(EPSR))*KC
 97          PRINT 1050,DISP
 98          READ(6,*,END=40) TEMP
 99          DISP=TEMP
100 40       REWIND 6
101          GAMMA=CSQRT(KC*KC-EPSR*(1.0-J*DISP)*KO*KO)
102          ALPHA=REAL(GAMMA)
103          ALPDB=20.0*A1*ALPHA
104          ATTEN=ALPDB*LENGTH
105          PRINT 1060,ALPHA,ALPDB
106          PRINT 1065,ATTEN
107          WRITE(3,*) FREQ,ATTEN
108          PRINT 2020
109          TEMP=FREQ
110          PRINT 1070,FREQ
111          PRINT 1080
112          READ(6,*,END=20) TEMP
113          FREQ=TEMP
114          IF(FREQ.NE.0.0) GO TO 20
115          CLOSE(3)
116          IF(NAME.NE.'OUTPF') CALL PF('SAVE',NAME)
117          STOP
118 1000     FORMAT('ENTER PIPE RADIUS IN CM')
119 1010     FORMAT('ENTER PIPE LENGTH IN CM')
120 1020     FORMAT('ENTER THE OUPUT FILE NAME, (DEFAULT OUTPF)')
121 1030     FORMAT('ENTER THE FREQUENCY IN GHZ')
122 1040     FORMAT('ENTER THE DIELECTRIC CONSTANT, DEFAULT ',F6.2)
123 1050     FORMAT('ENTER THE LOSS TANGENT, DEFAULT ',F5.3)
124 1060     FORMAT(//'  ALPHA = ',1P1E10.3,' NEPERS/CM   (',0PF5.2,' DB)')
125 1065     FORMAT('  TOTAL ATTENUATION = ',F7.2,' DB')
126 1070     FORMAT('ENTER THE FREQUENCY IN GHZ, DEFAULT ',F8.3)
127 1080     FORMAT('ENTER 0 TO QUIT')
128 2010     FORMAT(A7)
129 2020     FORMAT(//'-----------------------------------------')
130          END
```

Figure C2. (Cont'd).

$$f_c = \frac{c\, h_{nm}}{2\pi\sqrt{\varepsilon_r}} \qquad \text{[Eq C5]}$$

where ε_r is the relative dielectric constant of the material in the waveguide. Because only the real part of γ^2 is used to define cutoff, the loss tangent (the imaginary part of the complex permittivity) is neglected.

γ is computed at line number 98 in program Pipe 1A (line number 101 in program Pipe 1B). The program variables used in the computation of γ are defined in Table C1. Both programs use the same variables, so only one table is presented. The overall attenuation in dB resulting from the length of pipe is computed at line number 101 (104) in program Pipe 1A (Pipe 1B).

A sample run of each program for distilled water is presented in Figures C3 and C4. A pipe of radius 1.0 in. (2.54 cm) and length 6 in. (15.24 cm) was modeled. Table C2 lists the relative dielectric constants and loss tangents used for the frequency band of 1.0 to 10.0 GHz. These values were interpolated linearly from data given by von Hippel for 300 MHz, 3 GHz, and 10 GHz.[9] Because Program Pipe 1A uses one relative dielectric constant and one loss tangent for a band of frequencies, the average value of these parameters over the frequency band of 1.0 GHz to 10 GHz was used.

Table C3 is a summary of the attenuation output data generated by these programs. Note that between 1 and 5 GHz, Pipe 1B predicts less attenuation than Pipe 1A and vice-versa between 6 and 10 GHz. This occurs because attenuation is very dependent on loss tangent. Between 1 and 5 GHz, the loss tangent used by Pipe 1A is greater than that used by Pipe 1B, resulting in greater attenuation. Between 6 and 10 GHz, the loss tangent used by Pipe 1A is less than that used by Pipe 1B, resulting in less attenuation.

[9] A. R. von Hippel.

Table C1

Variables Used in Programs Pipe 1A and Pipe 1B

Variable	Definition	Line nos. where defined (Pipe 1A, Pipe 1B)
A1	$\text{Log}_{10}\ e$	66,73
DISP	tan δ, Loss tangent	76,98
EPSR	ϵ_r, Relative dielectric constant	73,93
FREQ	f, Frequency in GHz	96,(89 or 112)
J	j, $\sqrt{-1}$	64,71
LENGTH	l, Length of pipe in cm	71,80
PI	π	63,70
P11P	$(ha)_{nm}$ for TE_{11} mode	65,72
RADIUS	r, Radius of pipe in cm	68,77
KC	k_c, $(ha)_{11}/r$ (r in cm)	69,78
KO	k_o, $2\pi f/30$ (f in GHz)	97,91
GAMMA	$\gamma = \sqrt{k_c^2 - \epsilon_r (1 - j\tan\delta) k_o^2}$	98,101
ALPHA	α, Real part of γ	99,102
ALPDB	Attenuation in $\frac{dB}{cm}$, $20\ \text{Log}_{10} e^{\alpha}$	100,103
ATTEN	Overall attenuation in dB, ALPDB x l	101,104
FC	Cutoff frequency, $\frac{1}{2\pi} \frac{29.997925}{\sqrt{\epsilon_r}} k_c$	74,96

Table C2

Relative Dielectric Constants and Loss Tangents for Distilled Water at 25°C

Frequency (GHz)	Relative dielectric constant (ϵ_r)	Loss tangent (tan δ)
1.0	77.3	.052
2.0	77.0	.105
3.0	76.7	.157
4.0	73.6	.212
5.0	70.5	.266
6.0	67.4	.321
7.0	64.3	.376
8.0	61.2	.430
9.0	58.1	.485
10.0	55.0	.540

$\overline{\epsilon_r} = 68.11$ $\qquad$ $\overline{\tan\delta} = .294$

```
 TERMINAL:   140
 83/08/25. 10.58.29.
U OF I CYBER 175-175 ACCOUNTS ONLY      NOS 1.4 - 501/498.

SIGNON: JKEMVUJ
PASSWORD
********
TERMINAL:    140, TTY
RECOVER/ CHARGE: -CERL

 LAST RECORDED SIGNON AT 16:03 08/24/83
** BEGIN CERL BILLING **
/GET,PIPE1A
/R.FTN5,I=PIPE1A,L=0
     0.147 CP SECONDS COMPILATION TIME.
/LGO
ENTER PIPE RADIUS IN CM
? 2.54
ENTER PIPE LENGTH IN CM
? 15.24
ENTER DIELECTRIC CONSTANT
? 68.11
ENTER THE LOSS TANGENT
? .294
ENTER MINIMUM FREQUENCY IN GHZ
? 1.0
ENTER MAXIMUM FREQUENCY IN GHZ
? 10.0
ENTER FREQUENCY INCREMENT IN GHZ
? 1.0
ENTER THE OUPUT FILE NAME, (DEFAULT OUTPF)
? WATER
-------------------------------------------------------------

RADIUS =   2.540 CM     LENGTH =   15.240 CM
EPSILON =  68.11        LOSS TANGENT =  .2940

  CUTOFF FREQUENCY =    .419 GHZ

   FREQ (GHZ)   ALPHA (NEPERS/CM)   ALPHA (DB/CM)   ATTEN (DB)
   ------------------------------------------------------------
      1.00          2.757E-01          2.39          36.49
      2.00          5.138E-01          4.46          68.02
      3.00          7.615E-01          6.61         100.80
      4.00          1.011E+00          8.78         133.84
      5.00          1.261E+00         10.96         166.98
      6.00          1.512E+00         13.13         200.17
      7.00          1.763E+00         15.31         233.39
      8.00          2.014E+00         17.49         266.62
      9.00          2.265E+00         19.68         299.87
     10.00          2.517E+00         21.86         333.12
-------------------------------------------------------------
     0.036 CP SECONDS EXECUTION TIME.
```

Figure C3. Sample run of program Pipe 1A for distilled water.

```
 TERMINAL:   113
 83/08/25. 14.37.56.
U OF I CYBER 175-175 ACCOUNTS ONLY      NOS 1.4 - 501/498.


SIGNON: 3KEMVUJ
PASSWORD
********
TERMINAL:    113, TTY
RECOVER/ CHARGE: -CERL

 LAST RECORDED SIGNON AT 14:36 08/25/83
** BEGIN CERL BILLING **
/GET,PIPE1B
/R.FTN5,I=PIPE1B,L=0
     0.134 CP SECONDS COMPILATION TIME.
/LGO
ENTER PIPE RADIUS IN CM
? 2.54
ENTER PIPE LENGTH IN CM
? 15.24
ENTER THE OUPUT FILE NAME, (DEFAULT OUTPF)
? WATER2

-------------------------------------------


ENTER THE FREQUENCY IN GHZ
? 1.0
ENTER THE DIELECTRIC CONSTANT, DEFAULT   1.00
? 77.3
ENTER THE LOSS TANGENT, DEFAULT 0.000
? .052


  ALPHA =  5.206E-02 NEPERS/CM   (  .45 DB)
  TOTAL ATTENUATION =    6.89 DB


-------------------------------------------


ENTER THE FREQUENCY IN GHZ, DEFAULT    1.000
ENTER 0 TO QUIT
? 2.0
ENTER THE DIELECTRIC CONSTANT, DEFAULT  77.30
? 77.0
ENTER THE LOSS TANGENT, DEFAULT  .052
? .105


  ALPHA =  1.965E-01 NEPERS/CM   ( 1.71 DB)
  TOTAL ATTENUATION =   26.02 DB
```

Figure C4. Sample run of Program Pipe 1B for distilled water.

```
ENTER THE FREQUENCY IN GHZ, DEFAULT    2.000
ENTER 0 TO QUIT
? 3.0
ENTER THE DIELECTRIC CONSTANT, DEFAULT  77.00
? 76.7
ENTER THE LOSS TANGENT, DEFAULT  .105
? .157


  ALPHA =  4.344E-01 NEPERS/CM   ( 3.77 DB)
  TOTAL ATTENUATION =   57.50 DB


-------------------------------------------


ENTER THE FREQUENCY IN GHZ, DEFAULT    3.000
ENTER 0 TO QUIT
? 4.0
ENTER THE DIELECTRIC CONSTANT, DEFAULT  76.70
? 73.6
ENTER THE LOSS TANGENT, DEFAULT  .157
? .212


  ALPHA =  7.614E-01 NEPERS/CM   ( 6.61 DB)
  TOTAL ATTENUATION =  100.79 DB


-------------------------------------------


ENTER THE FREQUENCY IN GHZ, DEFAULT    4.000
ENTER 0 TO QUIT
? 5.0
ENTER THE DIELECTRIC CONSTANT, DEFAULT  73.60
? 70.5
ENTER THE LOSS TANGENT, DEFAULT  .212
? .266


  ALPHA =  1.163E+00 NEPERS/CM   (10.10 DB)
  TOTAL ATTENUATION =  153.98 DB


-------------------------------------------


ENTER THE FREQUENCY IN GHZ, DEFAULT    5.000
ENTER 0 TO QUIT
? 6.0
ENTER THE DIELECTRIC CONSTANT, DEFAULT  70.50
? 67.4
ENTER THE LOSS TANGENT, DEFAULT  .266
? .321
```

Figure C4. (Cont'd).

```
  ALPHA =  1.639E+00 NEPERS/CM   (14.24 DB)
  TOTAL ATTENUATION =  216.99 DB


-------------------------------------------


ENTER THE FREQUENCY IN GHZ, DEFAULT    6.000
ENTER 0 TO QUIT
? 7.0
ENTER THE DIELECTRIC CONSTANT, DEFAULT  67.40
? 64.3
ENTER THE LOSS TANGENT, DEFAULT  .321
? .376


  ALPHA =  2.177E+00 NEPERS/CM   (18.91 DB)
  TOTAL ATTENUATION =  288.20 DB


-------------------------------------------


ENTER THE FREQUENCY IN GHZ, DEFAULT    7.000
ENTER 0 TO QUIT
? 8.0
ENTER THE DIELECTRIC CONSTANT, DEFAULT  64.30
? 61.2
ENTER THE LOSS TANGENT, DEFAULT  .376
? .43


  ALPHA =  2.762E+00 NEPERS/CM   (23.99 DB)
  TOTAL ATTENUATION =  365.57 DB


-------------------------------------------


ENTER THE FREQUENCY IN GHZ, DEFAULT    8.000
ENTER 0 TO QUIT
? 9.0
ENTER THE DIELECTRIC CONSTANT, DEFAULT  61.20
? 58.1
ENTER THE LOSS TANGENT, DEFAULT  .430
? .485
```

Figure C4. (Cont'd).

```
  ALPHA =  3.395E+00 NEPERS/CM   (29.49 DB)
  TOTAL ATTENUATION =  449.39 DB

-------------------------------------------


ENTER THE FREQUENCY IN GHZ, DEFAULT    9.000
ENTER 0 TO QUIT
? 10.0
ENTER THE DIELECTRIC CONSTANT, DEFAULT  58.10
? 55.0
ENTER THE LOSS TANGENT, DEFAULT  .485
? .54


  ALPHA =  4.061E+00 NEPERS/CM   (35.28 DB)
  TOTAL ATTENUATION =  537.63 DB


-------------------------------------------


ENTER THE FREQUENCY IN GHZ, DEFAULT   10.000
ENTER 0 TO QUIT
? 0
     0.062 CP SECONDS EXECUTION TIME.
/BYE

3KEMVUJ  COSTS:     61.219 SRUS AT $.0059 = $.36
```

Figure C4. (Cont'd).

Table C3

Summary of Output From Sample Runs*

Frequency (GHz)	Atten (dB) Pipe 1A (Constant ε_r and tan δ)	Pipe 1B (Variable ε_r and tan δ)
1.0	36.49	6.89
2.0	68.02	26.02
3.0	100.80	57.50
4.0	133.84	100.79
5.0	166.98	153.98
6.0	200.17	216.99
7.0	233.39	288.20
8.0	266.62	365.57
9.0	299.87	449.39
10.0	333.12	537.63

*See Figures C3 and C4.

APPENDIX D:

DETERMINATION OF MATERIAL PARAMETERS

There are few published measurements of the relative dielectric constant, ε_r, and the loss tangent, tan δ, in the microwave bands for fluids. Von Hippel provides data at discrete, widely spaced frequencies.[10] Since the relative dielectric constant varies slowly with frequency and does not have a great effect on the overall waveguide attenuation, an interpolated value can be used for ε_r. However, the same cannot be said for the loss tangent.

Accurate values of ε_r, and tan δ are required to realistically compare theory with experiment. In the microwave frequency band, loss tangents can vary widely with frequency and from sample to sample, depending on the purity of the sample. Most importantly, an accurate value for the loss tangent is needed. As shown in Chapter 3, a small variation in tan δ can result in a large change in waveguide attenuation.

Loss tangents were calculated using transmission measurements through a dielectric slab. The dielectric slab consisted of a plexiglass tank filled with the desired fluid. The interior thickness of the tank was 6 in. (15.24 cm). The walls consisted of 0.5-in. (1.27-cm)-thick plexiglass.

A transmitter and waveguide horn antenna were placed on one side of the tank, and a receiver and another waveguide horn antenna on the other side. Precautions such as placing the tank in a shielded enclosure wall were taken to reduce multipath effects.

Transmission measurements were referenced to free-space measurements over the same distance. This eliminated the error caused by power variation with frequency and minimized the error caused by variations in the waveguide horns' efficiency with frequency.

Knowing the relative dielectric constants of the plexiglass and fluid, the loss tangent of the plexiglass, and the thickness of the plexiglass and fluid, the loss tangent of the fluid from a transmitted power measurement can be calculated. The equations derived in Appendix F are used for this computation. These calculations were performed for three fluids: carbon tetrachloride, methanol, and distilled water.

In these calculations, the relative dielectric constant for plexiglass was assumed to be 2.5. The loss tangent for plexiglass was assumed to be 0. Relative dielectric constants of the fluids were interpolated from published measurements.[11]

[10] A. R. von Hippel.
[11] A. R. von Hippel.

Tables D1 through D3 list the measured values of tan δ along with the published values. The measured values of tan δ were consistently lower than the published values, except for carbon tetrachloride, for which the loss tangent was too small to measure by the above method. The discrepancy is probably explained by the nonideal conditions of the experiment. The theoretical analysis was based on plane wave propagation and infinite slabs whereas the measurements were performed with horn antennas and a finite slab.

To estimate a more accurate value of the loss tangent, the measured values of tan δ were used to show the trend (shape of the curve) of the data. The published data provide a reference level. The last column of Tables D1 and D2 contains the corrected values of loss tangents. For carbon tetrachloride, the published value was used throughout the band.

Table D1

Relative Dielectric Constant and Loss Tangent Data for Carbon Tetrachloride*

Frequency (GHz)	ε_r	tan δ		
		Published***	Measured**	Corrected
2.5	2.17			0.0004
3.0	2.17	0.0004		0.0004
3.5	2.17			0.0004
4.0	2.17			0.0004
4.5	2.17			0.0004
5.0	2.17			0.0004
5.5	2.17			0.0004
6.0	2.17			0.0004
6.5	2.17			0.0004
7.0	2.17			0.0004
7.5	2.17			0.0004
8.0	2.17			0.0004

*Relative dielectric constants obtained by interpolation.
**Unable to measure.
***From A. R. von Hippel.

Table D2

Relative Dielectric Constant and Loss Tangent Data for Methanol*

Frequency (GHz)	ε_r	tan δ		
		Published**	Measured	Corrected
3.0	23.9	0.640		
3.5				
4.0	24.0		0.218	0.234
4.5	24.0		0.199	0.215
5.0	24.0		0.173	0.189

Table D3

Relative Dielectric Constant and Loss Tangent Data for Distilled Water*

Frequency (GHz)	ε_r	tan δ		
		Published**	Measured	Corrected
2.5	76.8		0.136	0.152
3.0	76.7	0.157	0.141	0.157
3.5	73.6		0.147	0.163
4.0	70.9		0.126	0.142
4.5	68.5		0.111	0.127
5.0	66.4		0.087	0.104
5.5	64.5		0.071	0.087
6.0	62.7		0.064	0.080
6.5	61.1		0.058	0.074
7.0	59.6		0.062	0.078

*Relative dielectric constants were obtained by interpolation.
**From A. R. von Hippel.

APPENDIX E:

ATTENUATION OF ELECTROMAGNETIC WAVES BY A HONEYCOMB GRATING

Data showing the theoretical attenuation resulting from a honeycomb grating placed in a pipe are presented. The amount of attenuation depends on the grating size and the relative dielectric constant of the fluid in the pipe. A problem not addressed is the decrease in flow rate of the fluid as a result of the grating.

A computer program was developed to calculate the attenuation of an electromagnetic wave caused by a grating. The incident wave is taken to be normal to the grating. In addition to the attenuation caused by the waveguide below cutoff propagation, the attenuation caused by scattering at the interfaces is computed. Equation C1 in Appendix C is used to compute the loss from waveguide below cutoff propagation. The calculation of the loss due to scattering is complex, requiring spectral-domain analysis[12] and will not be discussed here.

Figure E1 is a drawing of the grating used in the analysis. The analysis was done for four fluids: carbon tetrachloride, methanol, distilled water, and air. Tables E1 through E4 list the attenuation result from scattering and waveguide below cutoff propagation for various frequencies between 2.5 and 7.6 GHz.

Note that the attenuation from scattering is minimal and can be neglected. This suggests a simpler method for analyzing the effects of gratings. Since most of the attenuation provided by a grating is caused by waveguide below cutoff propagation, the computer programs presented in Appendix C can be used to compute an attenuation factor. Because the grating thickness is usually much less than a wavelength, the single mode analysis used by programs Pipe 1A and Pipe 1B is only an approximation. Actual attenuation could be slighly higher or lower, depending on the amount of energy coupled into each mode.

In the simplest case, a grating can be viewed as a collection of waveguides. It is important to note that in this approximation, the total attenuation caused by the grating is equal to the attenuation from one cell (waveguide)--not to the sum of the individual cell attenuations.

---

[12] R. Mittra, R. Hall, and C. H. Tsao, "Spectral-Domain Analysis of Circular Patch Frequency Selective Surfaces (FSS)," IEEE Trans. Antenna Propagation, in press.

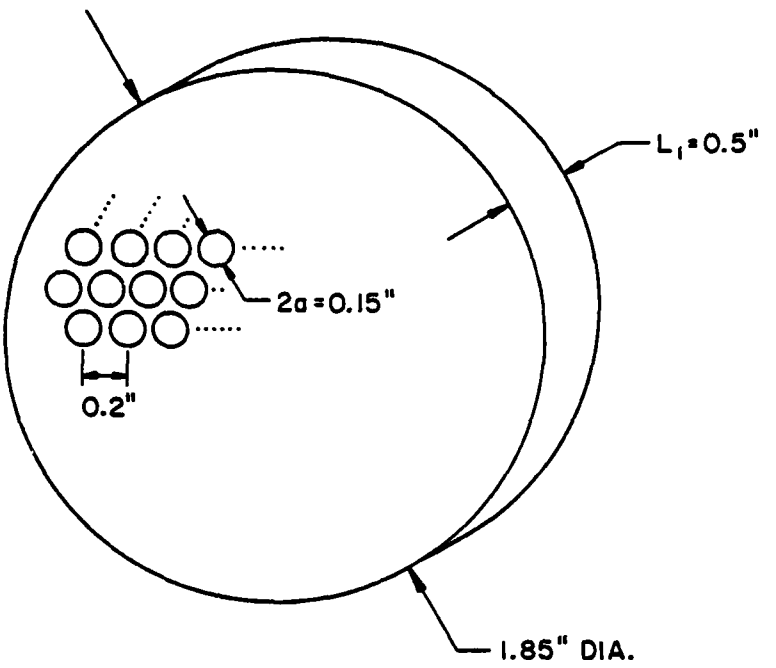

Figure E1. Diagram of the honeycomb grating used in calculating the attenuations in Tables E1, E2, E3, and E4.

Table E1

Calculated Attenuation Factors Resulting From a Honeycomb Grating: Carbon Tetrachloride

Frequency (GHz)	Attenuation from scattering	Attenuation from waveguide below cutoff propagation
2.5	.015	106.1
3.0	.024	106.0
3.5	.033	105.8
4.0	.044	105.6
4.5	.055	105.4
5.0	.068	105.1
5.5	.083	104.8
6.0	.099	104.5
6.5	.116	104.2
7.0	.135	103.8
7.5	.155	103.4

Table E2

Calculated Attenuation Factors Resulting From a Honeycomb Grating: Methanol

Frequency (GHz)	Attenuation from scattering	Attenuation from waveguide below cutoff propagation
4.0	.044	96.4
4.5	.055	93.6
5.0	.068	90.3

Table E3

Calculated Attenuation Factors Resulting From a Honeycomb Grating: Distilled Water

Frequency (GHz)	Attenuation from scattering	Attenuation from waveguide below cutoff propagation
2.5	.015	93.6
3.0	.024	87.5
3.5	.033	79.9
4.0	.044	70.3
4.5	.055	57.9
5.0	.068	40.6
5.5	.083	16.1
6.0	.099	11.1
6.5	.116	6.4
7.0	.135	6.4
7.5	.155	5.2
7.6	.159	5.0

Table E4

Calculated Attenuation Factors Resulting From a Honeycomb Grating: Air

Frequency (GHz)	Attenuation from scattering	Attenuation from waveguide below cutoff propagation
2.5	.015	106.3
3.0	.024	106.2
3.5	.033	106.2
4.0	.044	106.1
4.5	.055	106.0
5.0	.068	105.8
5.5	.083	105.7
6.0	.099	105.6
6.5	.116	105.4
7.0	.135	105.2
7.5	.155	105.1

APPENDIX F:

TRANSMISSION OF ELECTROMAGNETIC WAVES THROUGH MULTIPLE DIELECTRICS

Consider the problem of wave propagation through a multilayered dielectric region (Figure F1). Each layer has relative dielectric constant (possibly complex) $\epsilon_r = \epsilon_i$, $i = 1, 2, \ldots, N$ and lies between $z = z_{i-1}$ and z_i, where $z_0 = -\infty$ and $z_N = +\infty$. A TEM wave, propagating in the +z direction, is incident from the left. In the ith region, the electric and magnetic fields (E_i and H_i) are given by

$$E_i = T_i \left(e^{-jk_i z} + R_i e^{+jk_i z}\right) \qquad \text{[Eq F1]}$$

$$H_i = T_i Y_i \left(e^{-jk_i z} - R_i e^{+jk_i z}\right) \qquad \text{[Eq F2]}$$

where

$$Y_i = \sqrt{\epsilon_i}\, Y_o \qquad \text{[Eq F3]}$$

$$k_i = \sqrt{\epsilon_i}\, k_o \qquad \text{[Eq F4]}$$

Y_o and k_o are the free-space wave impedance and wave number, respectively. T_i is the transmission coefficient in the ith region. R_i is the ith reflection coefficient. Since regions 1 and N are unbounded, $T_i = 1$ and $R_N = 0$.

Forcing the continuity of E and H at the interface between the ith and the (i + 1)th layer, the following relationship results:

$$\begin{bmatrix} e^{-jk_i z_i} & e^{+jk_i z_i} \\ Y_i e^{-jk_i z_i} & -Y_i e^{+jk_i z_i} \end{bmatrix} \begin{bmatrix} T_i \\ T_i R_i \end{bmatrix} = \begin{bmatrix} e^{-jk_{i+1} z_i} & e^{+jk_{i+1} z_i} \\ Y_{i+1} e^{-jk_{i+1} z_i} & Y_{i+1} e^{+jk_{i+1} z_i} \end{bmatrix} \begin{bmatrix} T_{i+1} \\ T_{i+1} R_{i+1} \end{bmatrix} \qquad \text{[Eq F5]}$$

$i = 1, 2, \ldots, N-1$

If we then define:

$$X_i = \begin{bmatrix} T_i \\ T_i R_i \end{bmatrix} \qquad \text{[Eq F6]}$$

$$A_{i,j} = \begin{bmatrix} e^{-jk_i z_j} & e^{+jk_i z_j} \\ Y_i e^{-jk_i z_j} & -Y_i e^{+jk_i z_j} \end{bmatrix} \qquad \text{[Eq F7]}$$

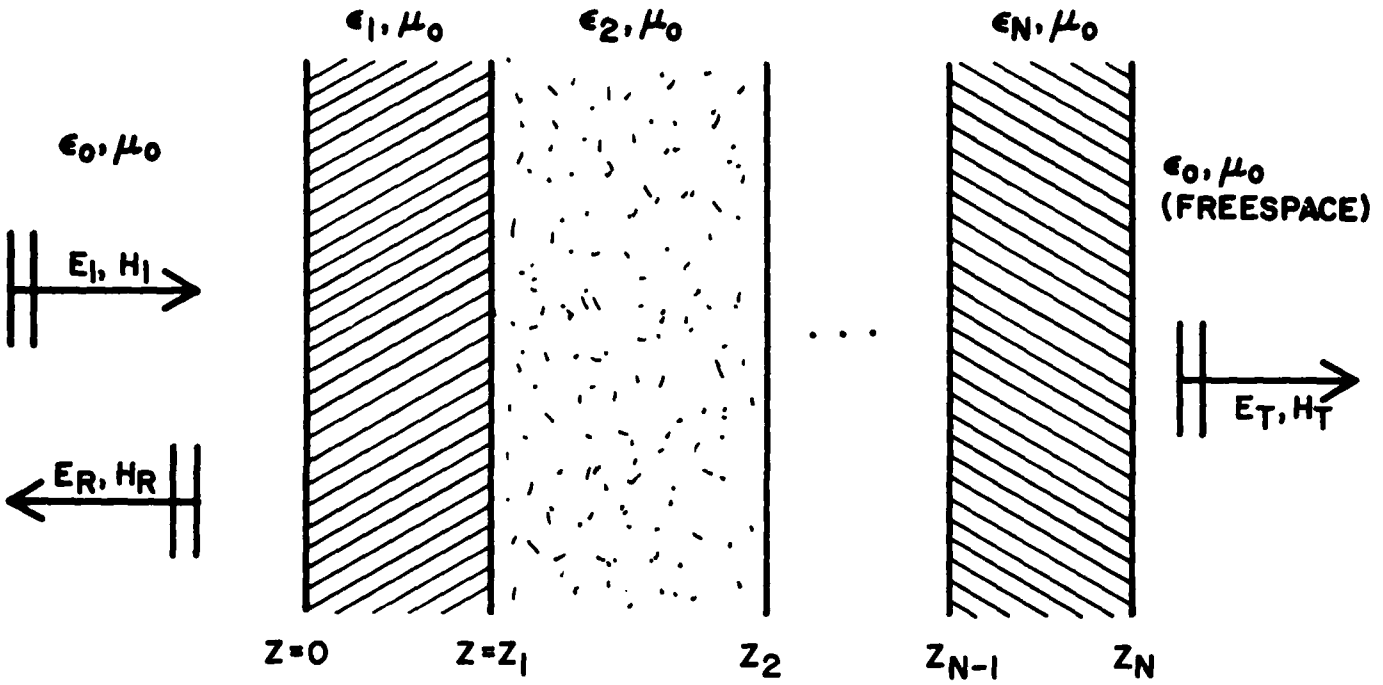

Figure F1. TEM wave propagation through a multilayered dielectric region.

Equation F4 can be rewritten as:

$$A_{i,i}\, X_i = A_{i+1,i}\, X_{i+1} \qquad i = 1, 2, \ldots, N-1 \qquad \text{[Eq F8]}$$

Solving for X_{i+1}:

$$(A_{i+1,i})^{-1}\, A_{i,i}\, X_i = X_{i+1} \qquad \text{[Eq F9]}$$

Equation F9 relates the reflection and transmission coefficients in the ith region to the reflection and transmission coefficients in the (i+1)th region by a matrix equation. These matrices can be cascaded to relate X_1 to X_N.

$$X_N = \left[\prod_{i=1}^{N-1} (A_{i+1,i})^{-1}\, A_{i,i} \right] X_i \qquad \text{[Eq F10]}$$

The bracketed quantity in Equation F10 is a 2x2 matrix, depending only on known quantities. As $T_1=1$ and $R_5=0$ for the dielectric slab measurement, Equation F10 consists of two equations and two unknowns, R_1 and T_5, the overall reflection and transmission coefficients. Equation F10 can be solved for R_1 and T_5. The matrix product in Equation F10 can be carried out analytically, although for large N values, this is difficult. It is often more convenient to calculate the matrix product numerically.

When one or more of the regions is particularly lossy and is more than several wavelengths long, certain numerical problems can arise in computing Equation F10. In this case, the $A_{i,i}$ matrices in the ith layer consist of both very large and very small numbers. To evaluate the matrix product in Equation F10, these numbers must be multiplied and added. This can yield inaccurate results when using finite precision arithmetic. This problem can be avoided

by using double precision arithmetic or using a computer with a longer word length. A second solution to the problem is obtained analytically by ignoring the heavily attenuated reflected terms.

CITED REFERENCES

Abramovitz, M., and I. Stegun, Handbook of Mathematical Functions (Dover Press, 1970).

Collin, R. F., Field Theory of Guided Waves (McGraw-Hill Co., 1960).

Collin, R. F., and F. J. Zucker, Antenna Theory, Part I (McGraw-Hill Co., 1969).

DASA EMP Handbook, DASA 2114-1 (Defense Atomic Support Agency [DASA] Information and Analysis Center, September 1968).

DNA EMP Awareness Course Notes, Third Ed., DNA 2172T (Defense Nuclear Agency, October 1977).

EMP Engineering Practices Handbook, NATO file No. 1460-2 (October 1977).

Kraus, J. D., Antennas (McGraw-Hill Co., 1950).

Marcuvity, N. (ed.), Waveguide Handbook (McGraw-Hill Co., 1951).

Measurement of Shielding Effectiveness of High-Performance Shielding Enclosures, Institute of Electrical and Electronic Engineers (IEEE) Method 299 (1975).

Method of Attenuation Measurements for Enclosures, Electromagnetic Shielding, for Electronic Test Purposes, MIL-STD-285 (Department of Defense, June 1975).

Mittra, R., R. Hall, and C. H. Tsao, "Spectral-Domain Analysis of Circular Patch Frequency Selective Surfaces (FSS)," IEEE Trans. Antenna Propagation, in press.

Nuclear Electromagnetic Pulse (NEMP) Protection, TM 5-855-5 (Headquarters, Department of the Army, February 1974).

Pearson, J. D., "The Diffraction of Electro-Magnetic Waves by a Semi-Infinite Circular Wave Guide," Proceedings of the Cambridge Philosophical Society, Vol 49, Part 4 (1953), pp 659-667.

Ramo, S., J. Whinnery, and T. Van Duzer, Fields and Waves in Communication Electronics (John Wiley and Sons, Inc., 1965).

Southworth, G. C., and A. P. King, "Metal Horns as Directive Receivers of Ultra-Short Waves," Proceedings of the I.R.E., Vol 27 (February 1939), pp 99-102.

von Hippel, A. R., Dielectric Materials and Applications (Technology Press of the Massachusetts Institute for Technology, 1954).

UNCITED REFERENCE

Decreton, M. C., and M. S. Ramachandraiah, "Nondestructive Measurement of Complex Permittivity for Dielectric Slabs," IEEE Transactions on Microwave Theory Technology (MTT) (December 1975), p 1077.

CERL DISTRIBUTION

Chief of Engineers
ATTN: Tech Monitor
ATTN: DAEN-ASI-L (2)
ATTN: DAEN-CCP
ATTN: DAEN-CW
ATTN: DAEN-CWE
ATTN: DAEN-CWM-R
ATTN: DAEN-CWO
ATTN: DAEN-CWP
ATTN: DAEN-EC
ATTN: DAEN-ECC
ATTN: DAEN-ECE
ATTN: DAEN-ZCF
ATTN: DAEN-ECR
ATTN: DAEN-RD
ATTN: DAEN-RDC
ATTN: DAEN-RDM
ATTN: DAEN-RM
ATTN: DAEN-ZCZ
ATTN: DAEN-ZCE
ATTN: DAEN-ZCI
ATTN: DAEN-ZCM

FESA, ATTN: Library 22060
ATTN: DET III 79906

US Army Engineer Districts
ATTN: Library (41)

US Army Engineer Divisions
ATTN: Library (14)

US Army Europe
AEAEN-ODCS/Engr 09403
ISAE 09081
V Corps
ATTN: DEH (11)
VII Corps
ATTN: DEH (15)
21st Support Command
ATTN: DEH (12)
USA Berlin
ATTN: DEH (15)
USASETAF
ATTN: DEH (6)
Allied Command Europe (ACE)
ATTN: DEH (3)

8th USA, Korea (14)

ROK/US Combined Forces Command 96301
ATTN: EUSA-HHC-CFC/Engr

USA Japan (USARJ)
ATTN: AJEN-FE 96343
ATTN: DEH-Honshu 96 '3
ATTN: DEH-Okinawa 96331

Area Engineer, AEDC-Area Office
Arnold Air Force Station, TN 37389

416th Engineer Command 60623
ATTN: Facilities Engineer

US Military Academy 10966
ATTN: Facilities Engineer
ATTN: Dept of Geography & Computer Science
ATTN: DSCPER/MAEN-A

AMMRC, ATTN: DRXMR-WE 02172

USA ARRCOM 61299
ATTN: DRCIS-RI-I
ATTN: DRSAR-IS

DARCOM - Dir., Inst., & Svcs.
ATTN: DEH (23)

DLA ATTN: DLA-WI 22314

FORSCOM
FORSCOM Engineer, ATTN: AFEN-DEH
ATTN: DEH (23)

HSC
ATTN: HSLO-F 78234
ATTN: Facilities Engineer
Fitzsimons AMC 80240
Walter Reed AMC 20012

INSCOM - Ch, Instl. Div.
ATTN: Facilities Engineer (3)

MDW
ATTN: DEH (3)

MTMC
ATTN: MTMC-SA 20315
ATTN: Facilities Engineer (3)

NARADCOM, ATTN: DRDNA-F 071160

TARCOM, Fac. Div. 48090

TRADOC
HQ, TRADOC, ATTN: ATEN-DEH
ATTN: DEH (19)

TSARCOM, ATTN: STSAS-F 63120

USACC
ATTN: Facilities Engineer (2)

WESTCOM
ATTN: DEH
Fort Shafter 96858
ATTN: APEN-IM

SHAPE 09055
ATTN: Survivability Section, CCB-OPS
Infrastructure Branch, LANDA

HQ USEUCOM 09128
ATTN: ECJ 4/7-LOE

U.S. Army, Fort Belvoir 22060
ATTN: Canadian Liaison Officer
ATTN: Water Resources Support Center
ATTN: Engr Studies Center
ATTN: Engr Topographic Lab
ATTN: ATZA-DTE-SU
ATTN: ATZA-DTE-EM
ATTN: R & D Command

CRREL, ATTN: Library 03755

WES, ATTN: Library 39180

HQ, XVIII Airborne Corps and
Ft. Bragg 28307
ATTN: AFZA-FE-EE

Chanute AFB, IL 61868
3345 CES/DE, Stop 27

Norton AFB CA 92409
ATTN: AFRCE-MX/DEE

Tyndall AFB, FL 32403
AFESC/Engineering & Service Lab

NAVFAC
ATTN: RDT&E Liaison Office (6)
ATTN: Sr. Tech. FAC-03T 22332
ATTN: Asst. COR R&D, FAC-03 22332

NCEL 93041
ATTN: Library (Code L08A)

Defense Technical Info. Center 22314
ATTN: DDA (12)

Engineering Societies Library
New York, NY 10017

National Guard Bureau 20310
Installation Division

US Government Printing Office 22304
Receiving Section/Depository Copies (2)

US Army Env. Hygiene Agency
ATTN: HSHB-E 21010

National Bureau of Standards 20760

EMS Team Distribution

Chief of Engineers 20314
ATTN: DAEN-MPZ-A
ATTN: DAEN-MPO-B
ATTN: DAEN-MPO-U

US Army Engineer District
New York 10007
ATTN: Chief, Design Br.
Pittsburgh 15222
ATTN: Chief, Engr Div
Philadelphia 19106
ATTN: Chief, NAPEN-D
Baltimore 21203
ATTN: Chief, Engr Div
Norfolk 23510
ATTN: Chief, NAOEN-M
ATTN: Chief, NAOEN-D
Huntington 25721
ATTN: Chief, ORHED-D
Wilmington 28401
ATTN: Chief, SAWEN-DS
ATTN: Chief, SAWEN-D
Charleston 29402
ATTN: Chief, Engr Div
Savannah 31402
ATTN: Chief, SASAS-L
Jacksonville 32232
ATTN: Const Div
ATTN: Design Br., Structures Sec.
Mobile 36628
ATTN: Chief, SAMEN-D
ATTN: Chief, SAMEN-C
Nashville 37202
ATTN: Chief, ORNED-D
Memphis 38103
ATTN: Chief, LMMED-DT
ATTN: Chief, LMMED-DM
Vicksburg 39180
ATTN: Chief, Engr Div
Louisville 40201
ATTN: Chief, Engr Div
Detroit 48231
ATTN: Chief, NCEED-T
St. Paul 55101
ATTN: Chief, ED-D
Chicago 60604
ATTN: Chief, NCCED-DS
Rock Island 61201
ATTN: Chief, Engr Div
ATTN: Chief, NCRED-D
St. Louis 63101
ATTN: Chief, ED-D
Kansas City 64106
ATTN: Chief, Engr Div
Omaha 68102
ATTN: Chief, Engr Div
New Orleans 70160
ATTN: Chief, LMNED-DG
Little Rock 72203
ATTN: Chief, Engr Div
Tulsa 74102
ATTN: Chief, Engr Div
Fort Worth 76102
ATTN: Chief, SWFED-D
Galveston 77550
ATTN: Chief, SWGAS-L
ATTN: Chief, SWGED-DS
ATTN: Chief, SWGED-DM
Albuquerque 87103
ATTN: Chief, Engr Div
Los Angeles 90053
ATTN: Chief, SPLED-D
San Francisco 94105
ATTN: Chief, Engr Div
Sacramento 95814
ATTN: Chief, SPKED-D
Far East 96301
ATTN: Chief, Engr Div
Portland 97208
ATTN: Chief, DB-6
ATTN: Chief, DB-3

US Army Engineer District
Seattle 98124
ATTN: Chief, NPSCO
ATTN: Chief, EN-DB-EM
ATTN: Chief, EN-DB-ST
ATTN: Chief, NPSEN-PL-WC
Walla Walla 99362
ATTN: Chief, Engr Div
Alaska 99501
ATTN: Chief, NPASA-R

US Army Engineer Division
New England 02154
ATTN: Chief, NEDED-T
Middle East (Rear) 22601
ATTN: Chief, MEDED-T
North Atlantic 10007
ATTN: Chief, NADEN-T
South Atlantic 30303
ATTN: Chief, SADEN-TS
ATTN: Chief, SADEN-TE/TM
Huntsville 35807
ATTN: Chief, HNDED-CS
ATTN: Chief, HNDED-ME
ATTN: Chief, HNDED-SR
ATTN: Chief, HNDED-FD
Ohio River 45201
ATTN: Chief, Engr Div
North Central 60605
ATTN: Chief, Engr Div
Missouri River 68101
ATTN: Chief, MRDED-T
Southwestern 75202
ATTN: Chief, SWDED-TS
ATTN: Chief, SWDED-TM
South Pacific 94111
ATTN: Chief, SPDED-TG
Pacific Ocean 96858
ATTN: Chief, Engr Div
ATTN: Chief, FM&S Branch
ATTN: Chief, PODED-D
North Pacific 97208
ATTN: Chief, Engr Div

6th US Army 94129
ATTN: AFKC-EN

7th US Army 09407
ATTN: AETTM-HRD-EHD

HQ, Combined Field Army (ROK/US) 96358
ATTN: CFAR-EN

US Army Foreign Science & Tech. Center
ATTN: Charlottesville, VA 22901
ATTN: Far East Office 96328

USA Liaison Detachment 10007
ATTN: Library

USA ARRADCOM 07801
ATTN: DRDAR-LCA-OK

CERCOM, Ft. Monmouth 07703
ATTN: DRSEL-LE-SS

Defense Nuclear Agency 20305
ATTN: DNA-RAEE
ATTN: DNA-STRA
ATTN: DNA-DDST
ATTN: DNA-RAEV

SHAPE 09055
Chief, Land & Msl. Instl. Section

Ft. Belvoir, VA 22060
ATTN: Learning Resources Center
ATTN: ATSE-TD-TL (2)

Fort Clayton, Canal Zone 34004
ATTN: DFAE

Ft. Leavenworth, KS 66027
ATTN: ATZLCA-SA

Ft. Lee, VA 23801
ATTN: DRXMC-D (2)

Ft. McPherson, GA 30330
ATTN: AFEN-CD

Ft. Monroe, VA 23651
ATTN: ATEN-AD (3)
ATTN: ATEN-FE-BG (2)
ATTN: ATEN-FE-W

Aberdeen Proving Ground, MD 21005
ATTN: AMXHE

Harry Diamond Labs 20783
ATTN: DELHD-NW-E
ATTN: DELHD-NW-EA
ATTN: DELHD-NW-EC
ATTN: DELHD-NW-ED
ATTN: DELHD-NW-EE

USA Natick Labs 01760
NARADCOM/DRDNA-UST

USA-WES 39180
ATTN: C/Structures

NAVFAC/Code 04
Alexandria, VA 22332

Naval Air Systems Command 20360
ATTN: Library

Naval Training Equipment Command 32813
ATTN: Technical Library

Port Hueneme, CA 93043
ATTN: Morell Library

Bolling AFB, DC 20332
AF/LEEEU

AFE, Camp Humphreys
APO San Francisco 96721

Griffiss AFB 13440
RADC/RBES

Hanscom AFB, MA 01731
ATTN: HQ AFSC
ATTN: ESD/OCR-3

Kirtland AFB, NM 87117
ATTN: AFWL/DES
ATTN: AFWL/DYC

Little Rock AFB 72076
ATTN: 314/DEEE

Patrick AFB, FL 32925
ATTN: XRQ

Tinker AFB, OK 73145
2854 ABG/DEEE

Tyndall AFB, FL 32403
ATTN: AFESC/TBT
ATTN: AFESC/RDCF

Wright-Patterson AFB, OH 45433
ATTN: ASD/ENAMA
ATTN: AFWAL/MLSE

Bldg. Research Advisory Board 20418
Dept. of Transportation Library 20590
Transportation Research Board 20418

Airports and Const. Services Dir.
Technical Info. Reference Centre
Ottawa, Canada K1A ON8

The effect of fluids on waveguides below cutoff penetrations as related to electromagnetic shielding effectiveness / by Michael K. McInerney ... (et al.) - Champaign, Ill : Construction Engineering Research Laboratory, 1984.
62 p. (Technical report / Construction Engineering Research Laboratory ; M-354).

1. Shielding (electricity). 2. Wave guides. 3. Fluids. I. McInerney, Michael K. II. Ray, Scott, III. McCormack, Raymond G. IV. Castillo, Steve. V. Mittra, Raj. VI. Series; Technical report (Construction Engineering Research Laboratory) ; M-354.